Electrical tests of the antenna for the production model of AN/MPQ-501

Allan, L.E.; Markell, R.C.; McCormick, G.C.

Report (National Research Council of Canada. Radio and Electrical Engineering Division : ERB), 1962-08

ERB - 624

CONFIDENTIAL

Copy 48

NATIONAL RESEARCH COUNCIL OF CANADA

RADIO AND ELECTRICAL ENGINEERING DIVISION

ELECTRICAL TESTS OF THE ANTENNA FOR THE PRODUCTION MODEL OF AN/MPQ - 501

L. E. ALLAN, R. C. MARKELL AND G. C. McCORMICK

OTTAWA

AUGUST 1962 NRC # 35657

ABSTRACT

The electrical tests of the antenna for the production model of the counter mortar radar, AN/MPQ-501, are reported. The VSWR was satisfactory. Representative patterns are shown. Beamwidths were 0.86° in azimuth in each beam; and in elevation, 0.84° for lower beam and 0.86° for upper beam. Side lobes are less than -20 db. Data regarding elevation beam position are presented; the beam separation is 39.6 mils at center of scan. The azimuth scan angle is proportional to rotor angle to within 0.5 mil. The gain of the antenna was 45.6 db at 16,000 mc/s at center of scan, and exceeded 45 db within the active limits of scan at all frequencies. Data with the production polarizer in place were obtained with respect to radiation patterns, gain, beam position, and axial ratio. The mean axial ratio was 0.95.

CONTENTS

PLATES

FIGURES

FIGURES

FIGURES

ELECTRICAL TESTS OF THE ANTENNA FOR THE PRODUCTION MODEL OF AN/MPQ-501

- L.E. Allan, R.C. Markell and G.C. McCormick -

INTRODUCTION

This report covers the antenna tests on the first production unit, Serial 1, of the Canadian counter mortar radar, AN/MPQ-501, carried out at the National Research Council during the spring and summer of 1962. The main purpose of the tests was to assess the electrical performance of the antenna before and after roading, in relation to what was specified [1,2] or anticipated. However, the tests were intended also to provide information useful in minor design modifications and in production and maintenance testing. The performance of the two earlier models has been reported previously [3,4]. They will be referred to, respectively, as the "McGill-NRC" model and the "NRC-CAL" model.

The antenna is basically a dual-beam Foster scanner [5,6] operating in the frequency band 15,840 mc/s to 16,160 mc/s. A pencil beam, approximately 0.9° by 0.9°, sweeps 20° in azimuth left to right on lower beam, then left to right on upper beam; then the cycle is repeated at the rate of 20 per second. The physical concepts involved in the operation of the scanner in order to perform this function are illustrated in Figs. 1, 2, and 3, which show the elevation geometry of the antenna, the scanner cross section, and the developed scanner regions. A photograph of the scanner antenna mounted for testing is shown in Plate I.

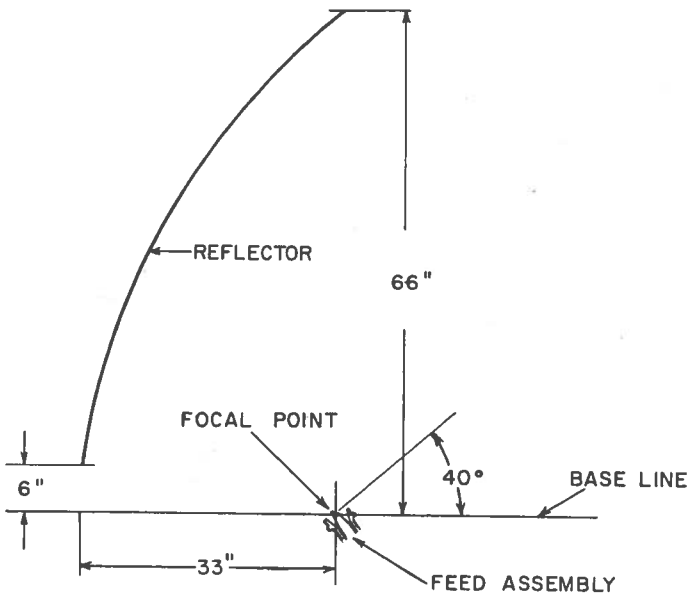

Fig. 1 Elevation geometry of the antenna

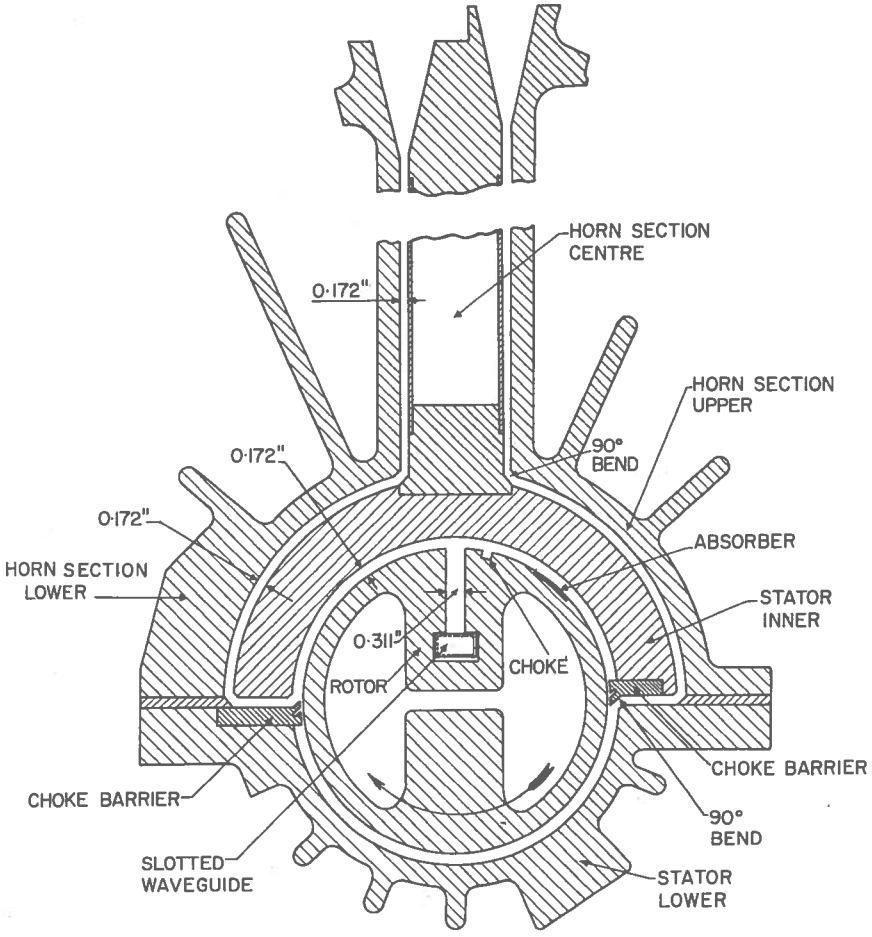

Fig. 2 Scanner cross section

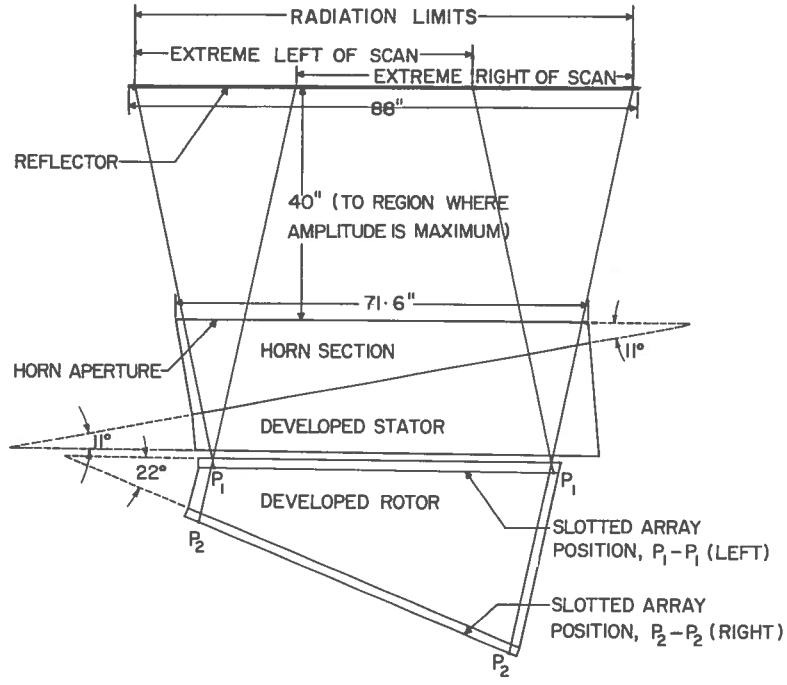

Fig. 3 Developed geometry of the scanner

A brief account of the history of the scanner has been published by Foster [5]. The design of the McGill-NRC model was carried out, for the most part, by Dr. Murray Telford at McGill University under Dr. Foster's general supervision. The NRC-CAL model manufactured by Canadian Arsenals Limited, and tested in 1957, incorporated several antenna modifications, notably the replacement of intermeshing teeth by a unity-coupled tee. Other changes in the McGill-NRC model for inclusion in the NRC-CAL model were made in the slotted array design, the slotted array region, and the dual horn assembly. Dr. Harry Gruenberg was responsible for the design of this model.

The most significant design change introduced in the production model was an extension to the horn-stator regions, the effect of which is that radiation at center of scan is propagated nearly normal to the horn assembly. The change in the horn assembly included the introduction of a heavy polyethylene cover to replace the $\frac{1}{32}$ inch Teflon sheet cover previously used. Horn dimensions were changed slightly in order to improve the match and in order to produce a beam separation closer to the nominal 40 mils* For convenient reference, a summary of certain antenna design features is contained in Appendix I.

The first part of the test schedule included the measurement of VSWR, gain, and beam position, and the recording of radiation patterns on the antenna as it was delivered from the manufacturer. There then followed the road tests, as called for in the specifications, carried out at the Canadian Army Proving Grounds. After the road tests the measurements listed above were repeated in order to assess the effect of roading. Pattern, gain, and beam position measurements were made with the polarizer in operating position, and polarization patterns were taken. The phase center of the antenna was located using a phase-sensitive four-horn device previously developed [7]. Also, from time to time, various features of the antenna or specific aspects of antenna performance were investigated in detail. Included in the latter category were a physical check of the feed-reflector geometry, an investigation of the occurrence of wide-angle reflection lobes, and means for the reduction of the first side lobe over lower beam.

VSWR

The VSWR of the antenna, including the rotating joint assembly, was measured at 15,840 mc/s, 16,000 mc/s, and 16,160 mc/s as a function of rotor position. The reflection coefficient was observed continuously with a reflectometer equipment as the rotor was turned. Measured values after roading are plotted in Figs. 4 to 6. Data obtained before roading differ only in minor details, except for generally lower peaks in the switch region. Rotor scale readings are related to scan angle as shown in Fig. 7.

---

* 1 mil = $\frac{360}{6400}$ degrees.

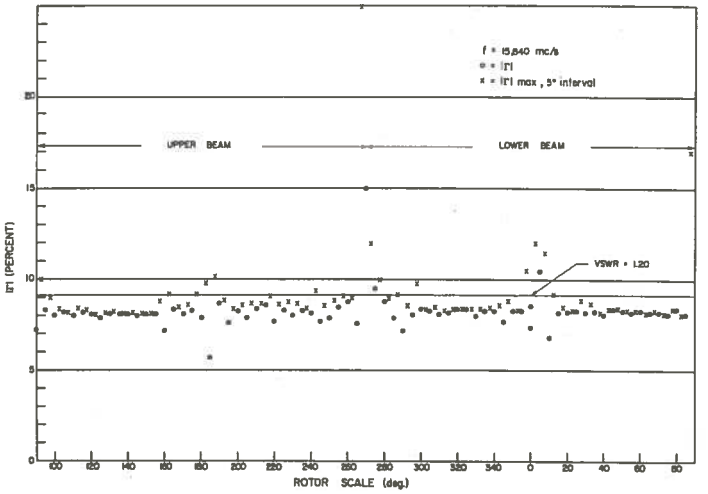

Fig. 4 Scanner reflection coefficient versus rotor position, $f = 15,840$ mc/s (after roading)

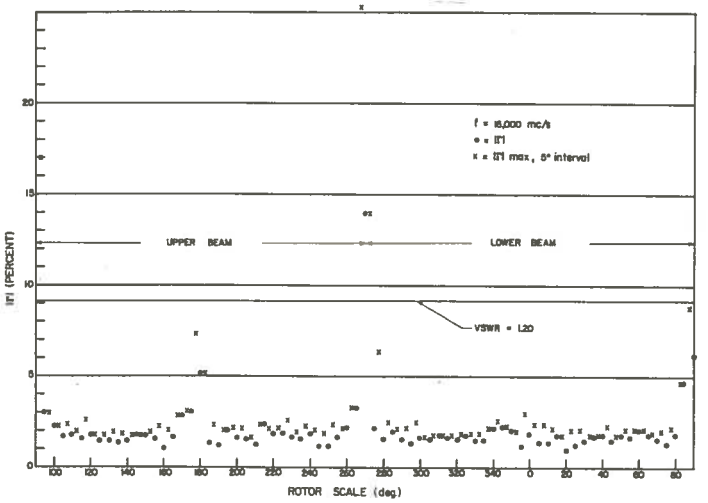

Fig. 5 Scanner reflection coefficient versus rotor position, $f = 16,000$ mc/s (after roading)

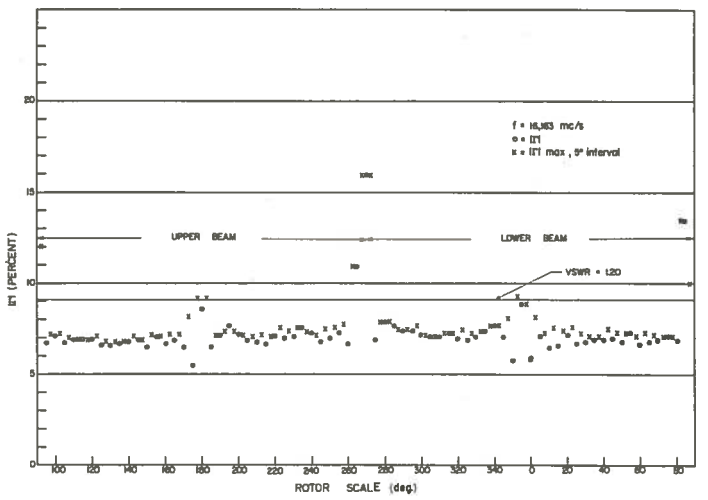

Fig. 6 Scanner reflection coefficient versus rotor position, $f = 16,160$ mc/s (after roading)

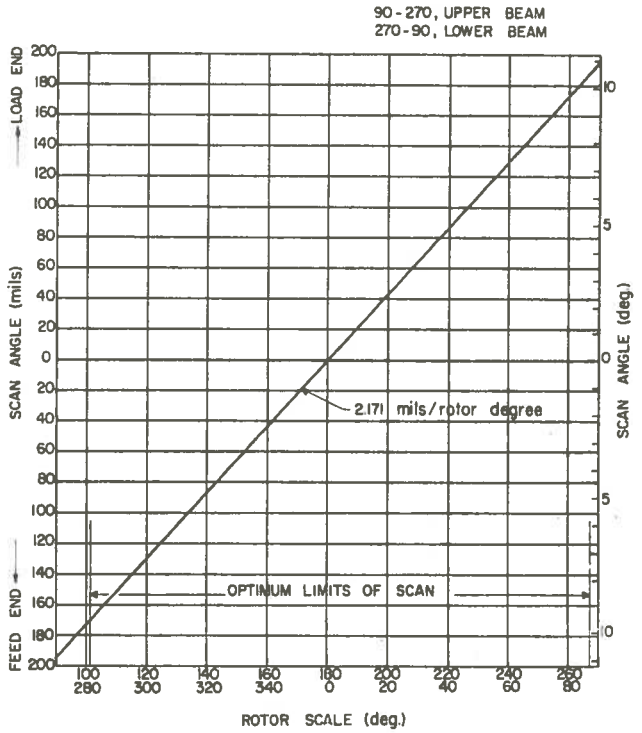

Fig. 7 Rotor scale versus scan angle for each beam with optimum limits of scan as shown

The VSWR level is constant over most of the rotor positions. This level is determined mainly by the rotating joint assembly which includes five E-plane bends as well as the joint*. Peaks in VSWR occur at special rotor positions; namely, the two switch regions where the scanner switches from lower beam to upper beam, and vice versa, and the two regions where radiation is normal to the scanner horns. In the former case a large percentage of the power is directed into the slotted waveguide termination, but some increase in VSWR can be expected. The maximum value observed before roading, in this region, was 1.54, and after roading, 1.98. Peaks at normal radiation are due to mismatches at the horn or within the scanner structure at discontinuities parallel to the phase front. They are, therefore, associated with the wide-angle side lobes to be discussed below, which are caused by internal reflections within the scanner. The height of the peak in the VSWR at this point is a reliable indication of the magnitude of the associated reflection lobe. The highest such rise in VSWR was from 1.05 to 1.16 on upper beam at 16,000 mc/s.

*A change in the fabrication of the E-plane bends has resulted in a reduction of the mean VSWR of the antenna to values well below the specified figure, 1.15.

PRIMARY PATTERNS

Primary patterns of each horn of the horn assembly were obtained at short range using the one-foot-long test section. These are shown in Fig. 8.

RECTANGULAR PATTERNS

The scanner antenna was mounted on a commercial azimuth-over-elevation positioner which was itself mounted on a heavy lower azimuth turntable. Patterns were recorded on a commercial decibel recorder with the klystron transmitter unit feeding a 5-foot parabolic antenna mounted on an 80-foot tower at a range of 2600 feet. Azimuth patterns were taken with the positioner azimuth axis perpendicular to line of sight. All patterns were taken with the scanner azimuth in the lock position. The antennas at both ends of the range were highly directive and no evidence of trouble due to ground reflections was observed. Most of the patterns were taken with a bolometer detector, although a calibrated crystal detector was occasionally used.

Representative patterns* before roading are shown in Figs. 10 to 19.

Beam Asymmetry

It will be seen from the patterns that the shape of the beam is asymmetrical in elevation for both the lower and upper beams. The asymmetry is present in all upper beam patterns and, in some, approaches the specified limit of 2 mils between the bisection of the 3 db points and the bisection of the 15 db points. The asymmetry of the lower beam results from a shoulder below the beam of magnitude 20 to 22 db. A less consistent asymmetry exists in azimuth patterns and is particularly noticeable near the limits of scan. The asymmetry as a function of signal level at center of scan is shown in Fig. 9.

Side Lobes

The occurrence of side lobes before roading is summarized immediately below.

i) Side Lobes : Elevation

a) Lower Beam Apart from a shoulder of -20 db to -22 db, side lobes under the beam were less than -30 db. A side lobe varying from -18.3 db to -21 db was observed immediately above the main beam.

b) Upper Beam Side lobes of -26 db to -30 db were observed below the beam and in the order of -28 db above the beam.

* The patterns reproduced in this report were selected from over 500 taken during the tests.

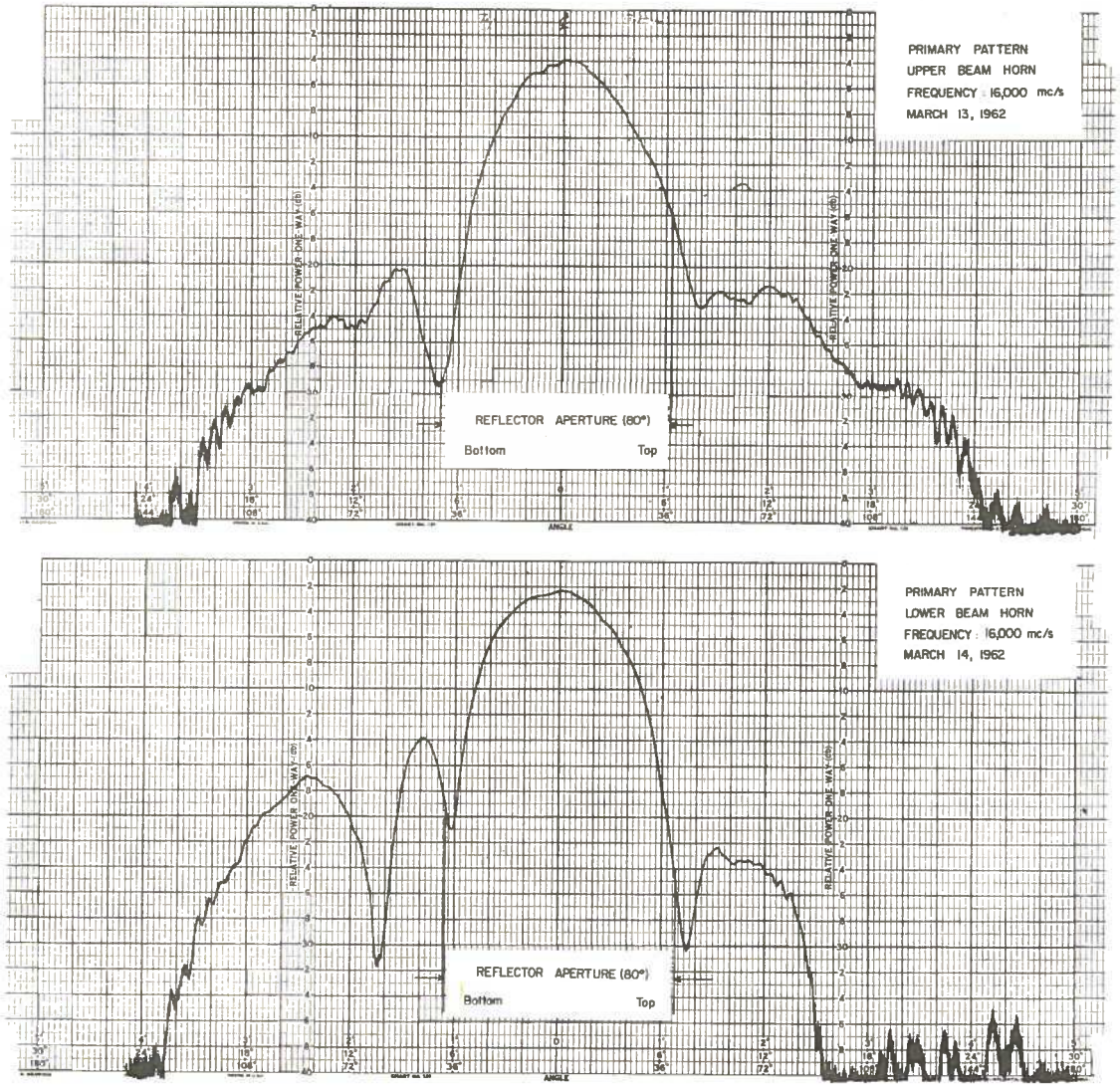

CONFIDENTIAL

Fig. 8 E-plane patterns (primary patterns) of horn assembly, $f = 16,000$ mc/s

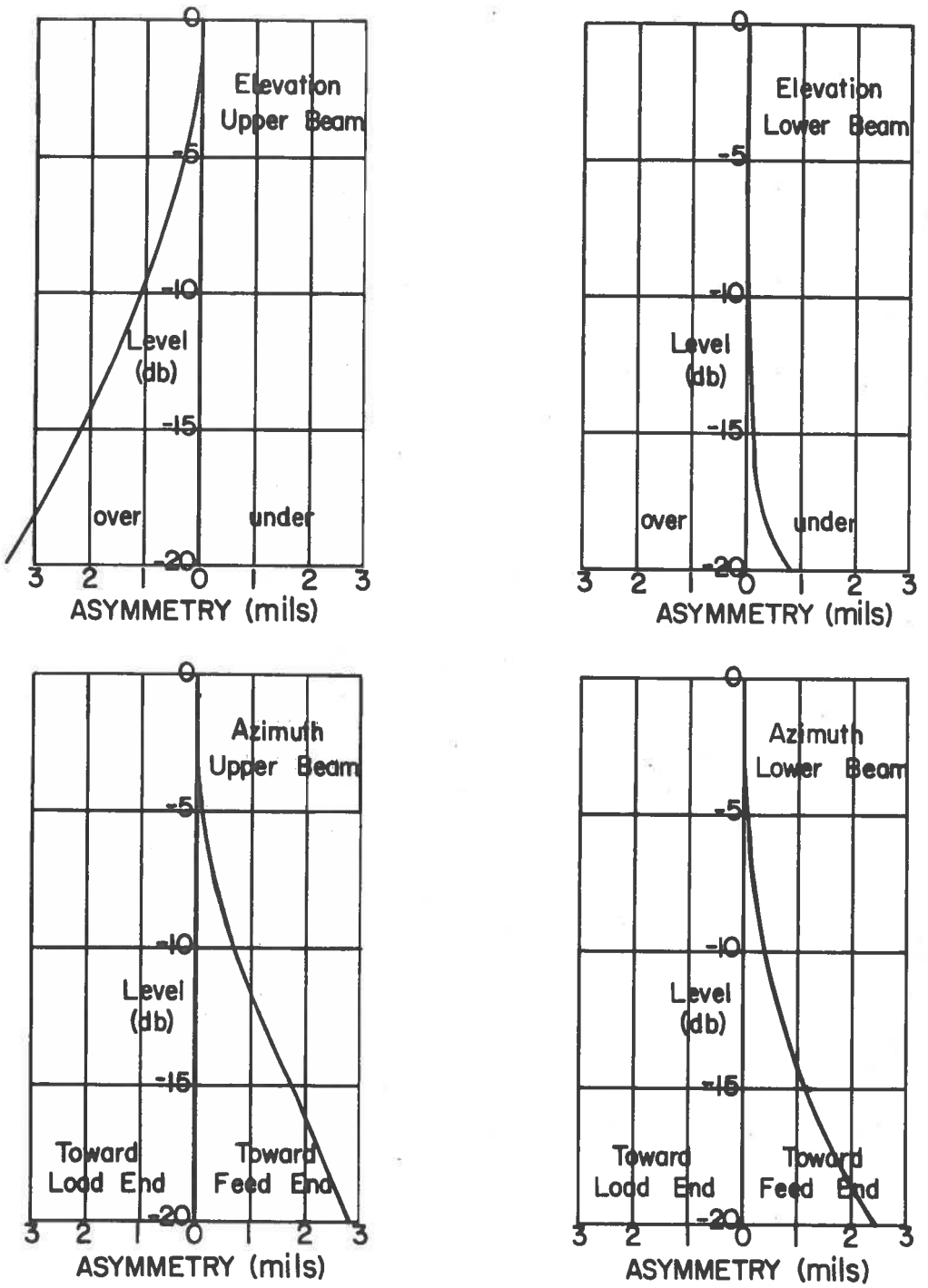

Fig. 9 Typical beam asymmetry. Scan angle = 0°, f = 16,000 mc/s

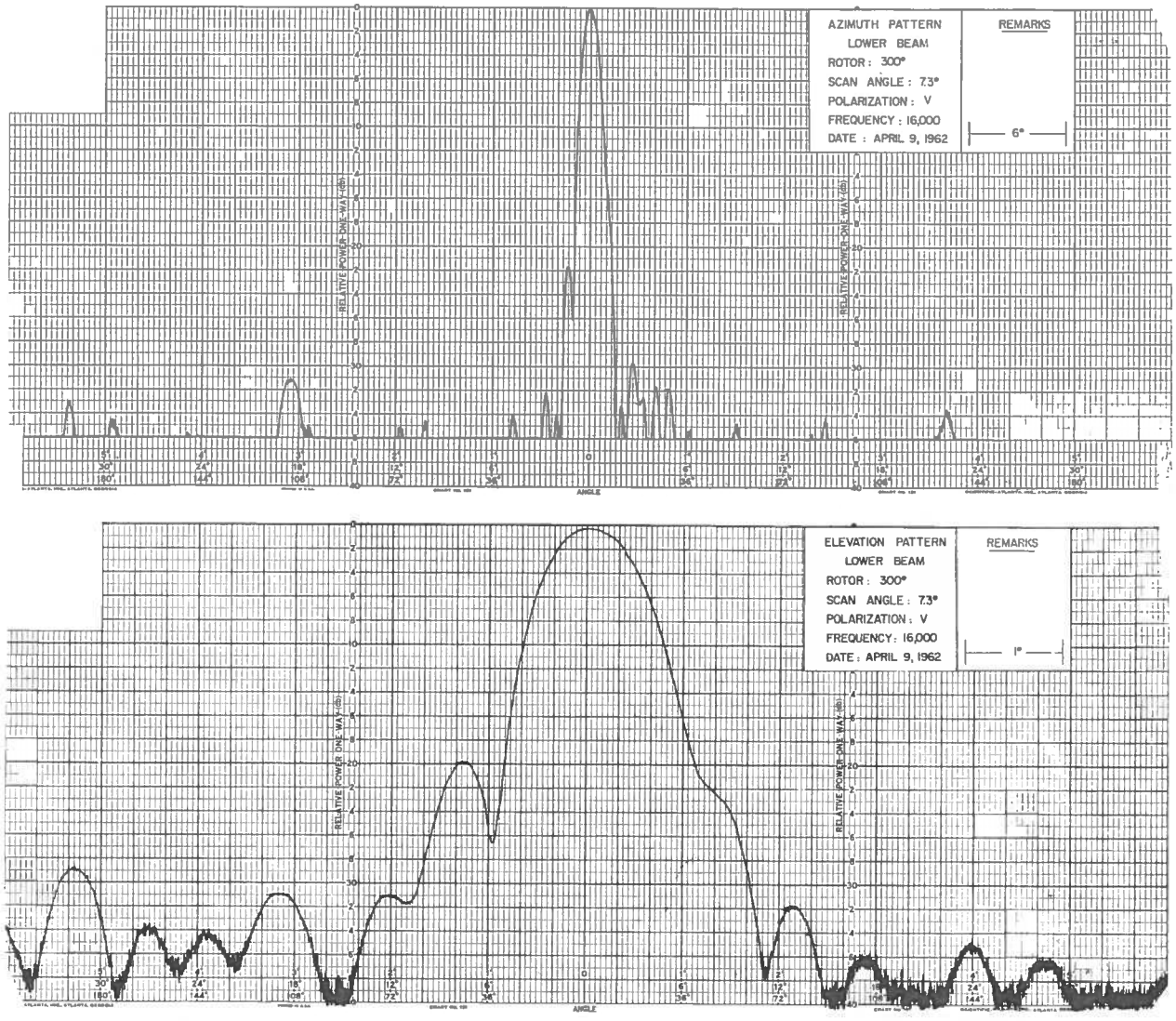

Fig. 10 Radiation patterns. $f = 16,000$ mc/s. Rotor = 300°. (before roading)

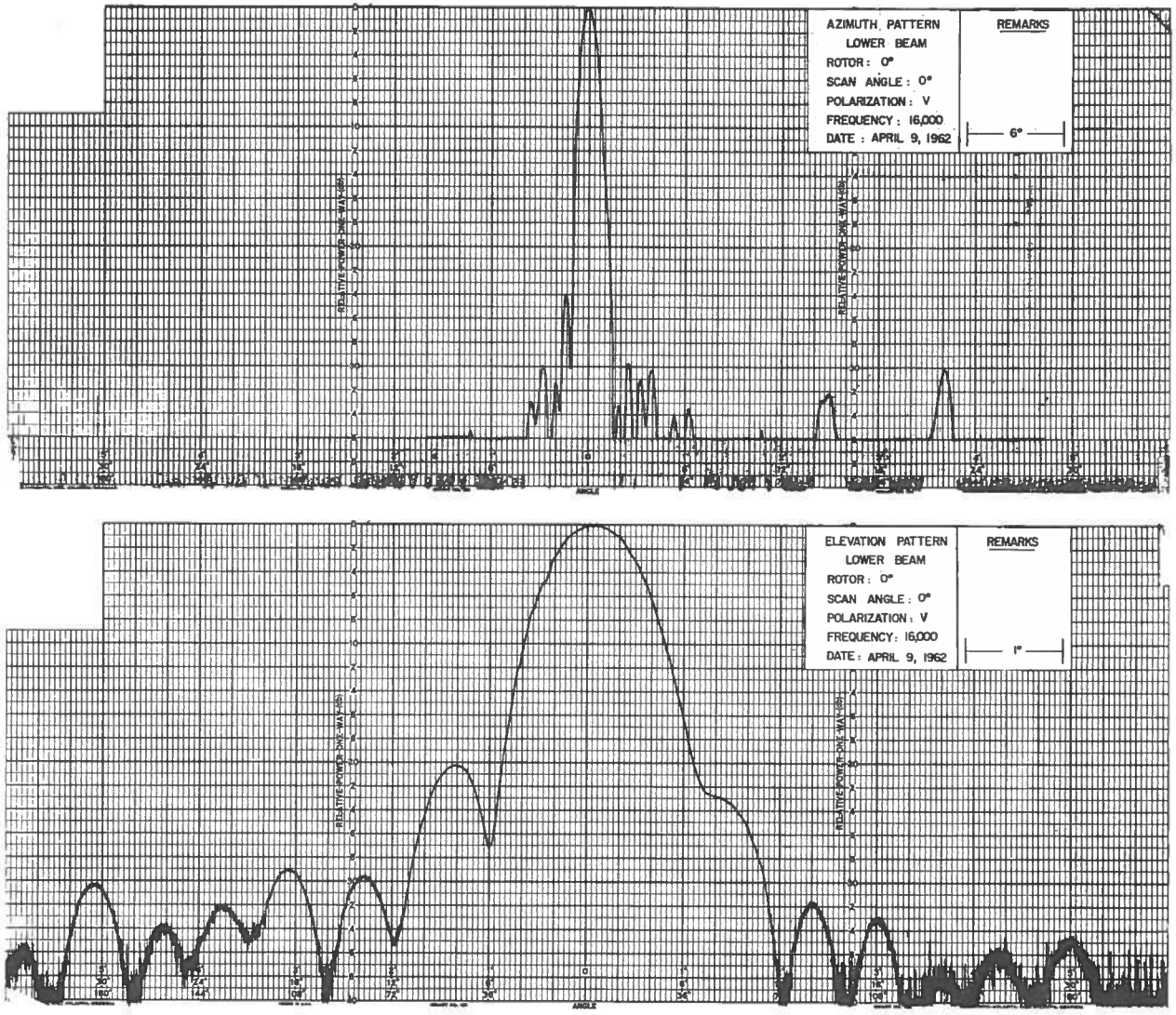

Fig. 11 Radiation patterns. $f = 16,000$ mc/s. Rotor = 0°. (before roading)

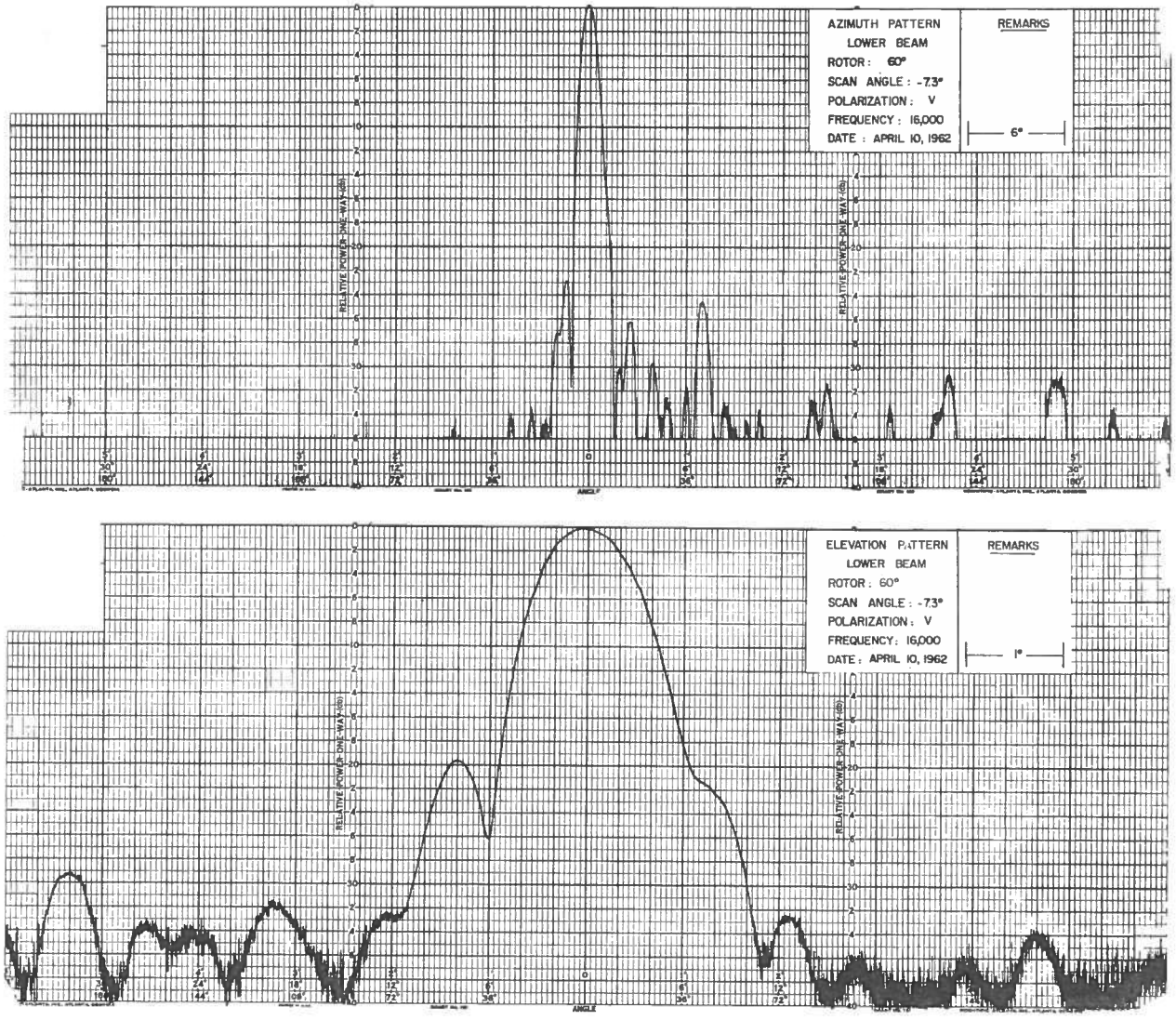

CONFIDENTIAL

Fig. 12 Radiation patterns. $f = 16,000$ mc/s. Rotor = 60°. (before roading)

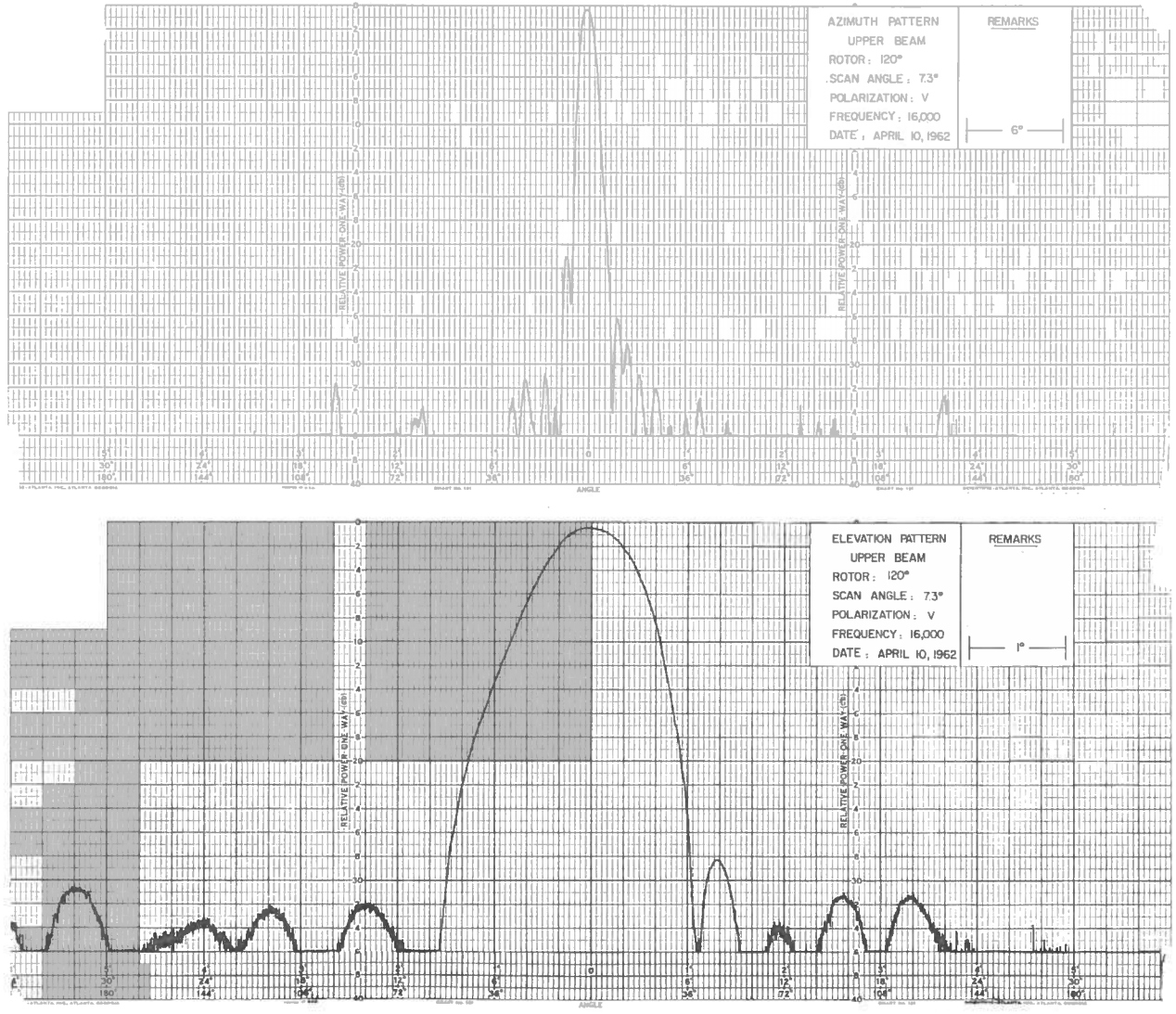

Fig. 13 Radiation patterns. $f = 16,000$ mc/s. Rotor = 120°. (before roading)

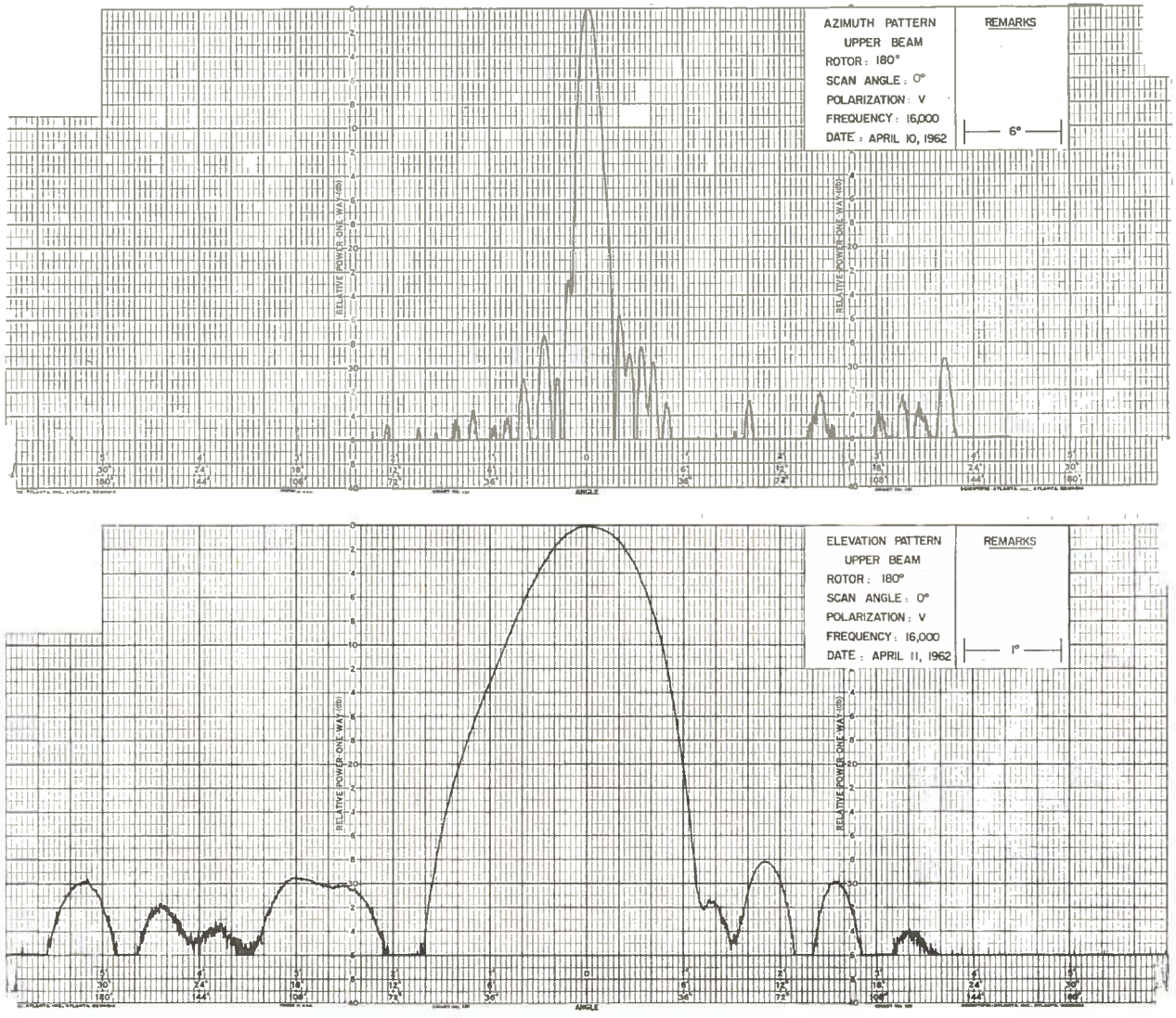

Fig. 14 Radiation patterns. $f = 16,000$ mc/s. Rotor = 180°. (before roading)

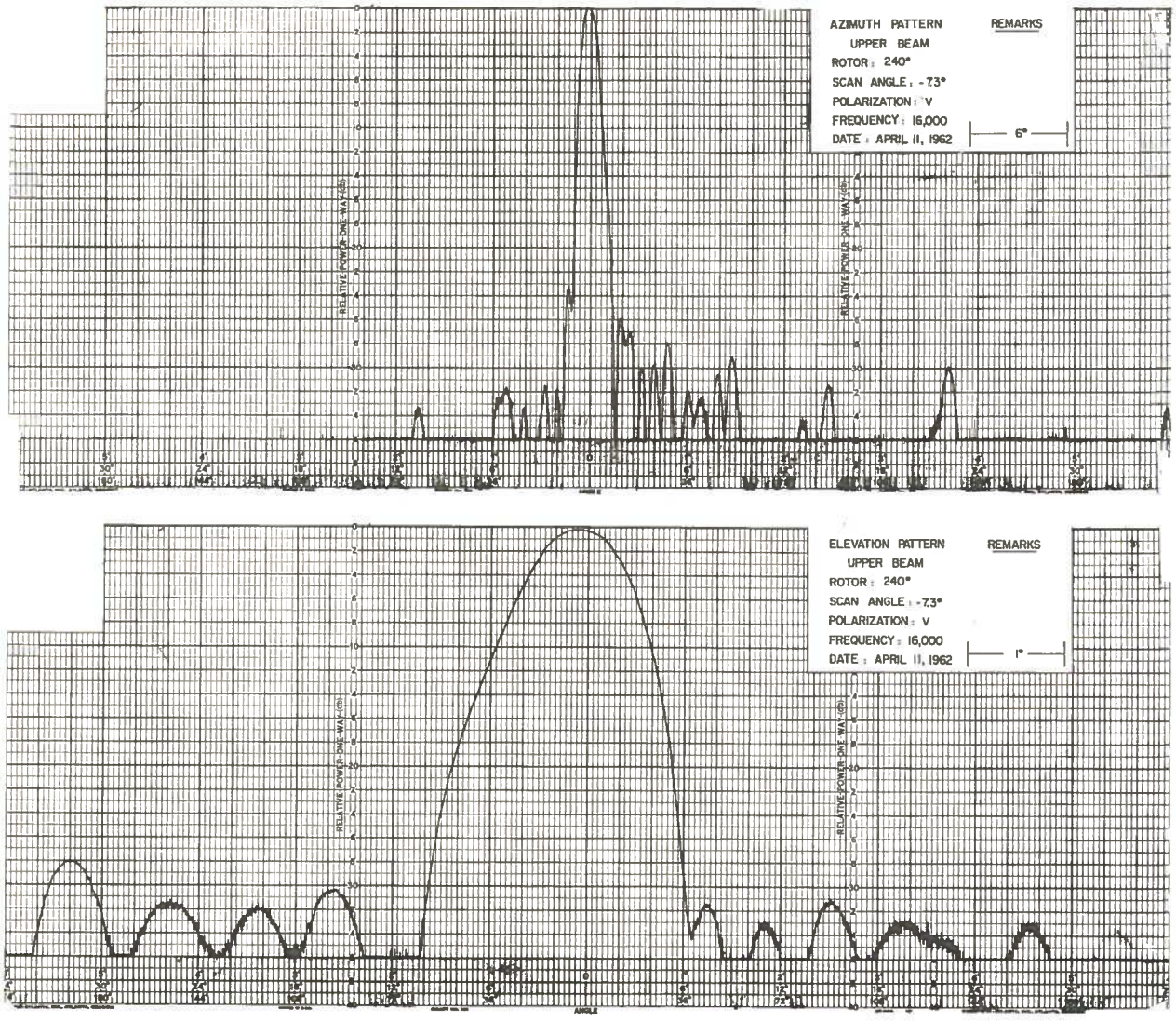

CONFIDENTIAL

Fig. 15 Radiation patterns. $f = 16,000$ mc/s. Rotor = 240°. (before roading)

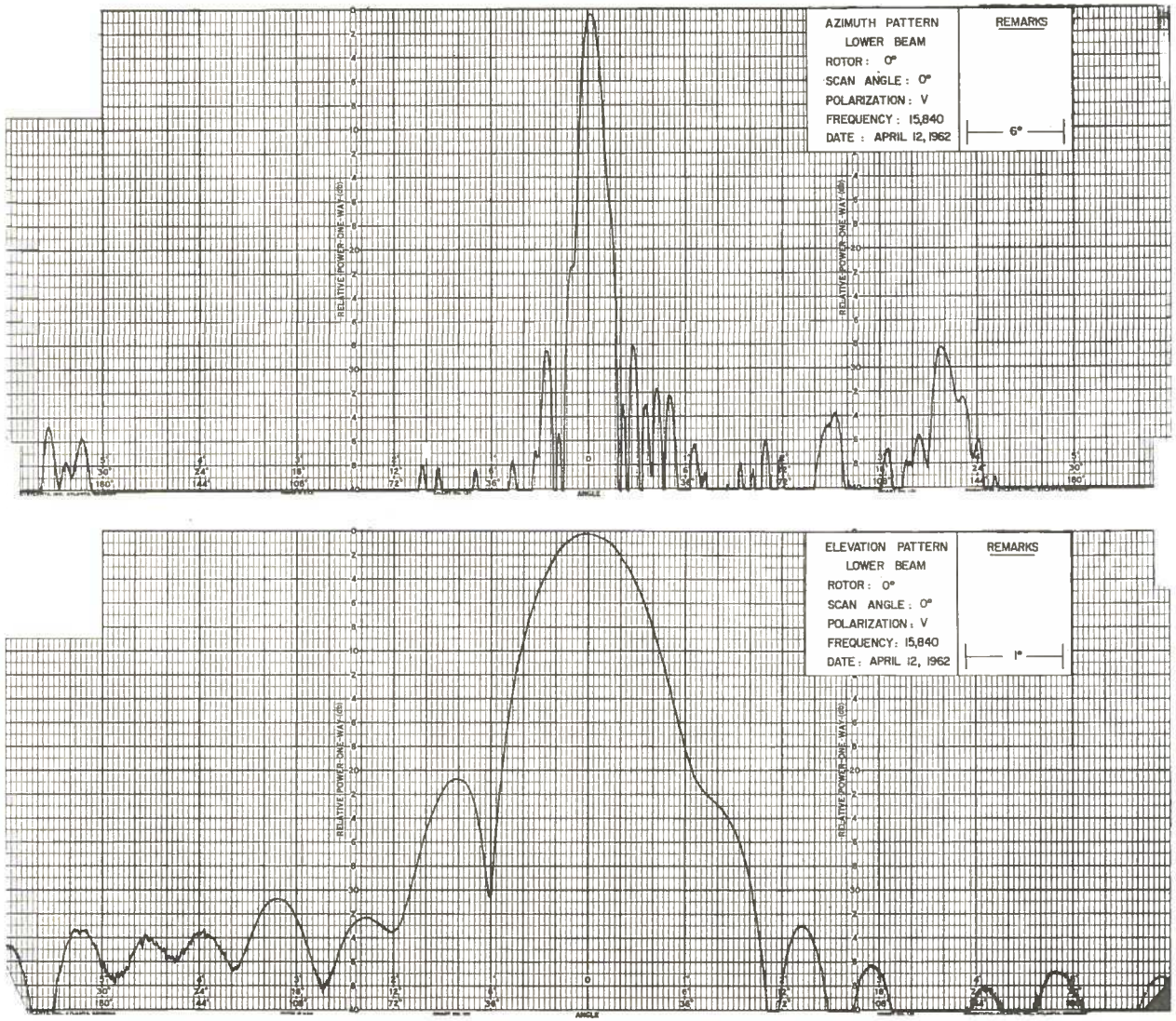

CONFIDENTIAL

Fig. 16 Radiation patterns. $f = 15,840$ mc/s. Rotor = 0°. (before roading)

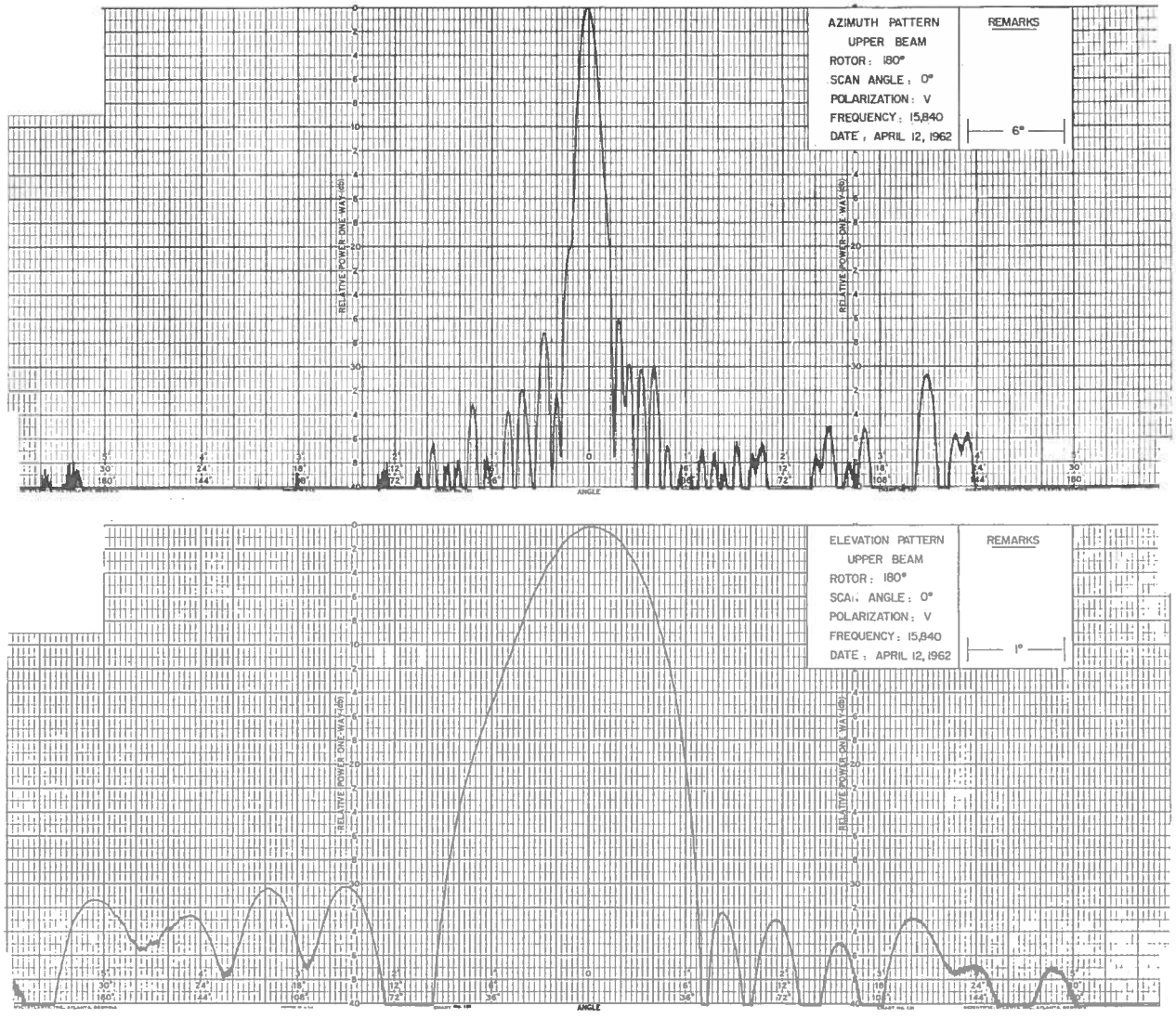

Fig. 17 Radiation patterns. $f = 15,840$ mc/s. Rotor = 180°. (before roading)

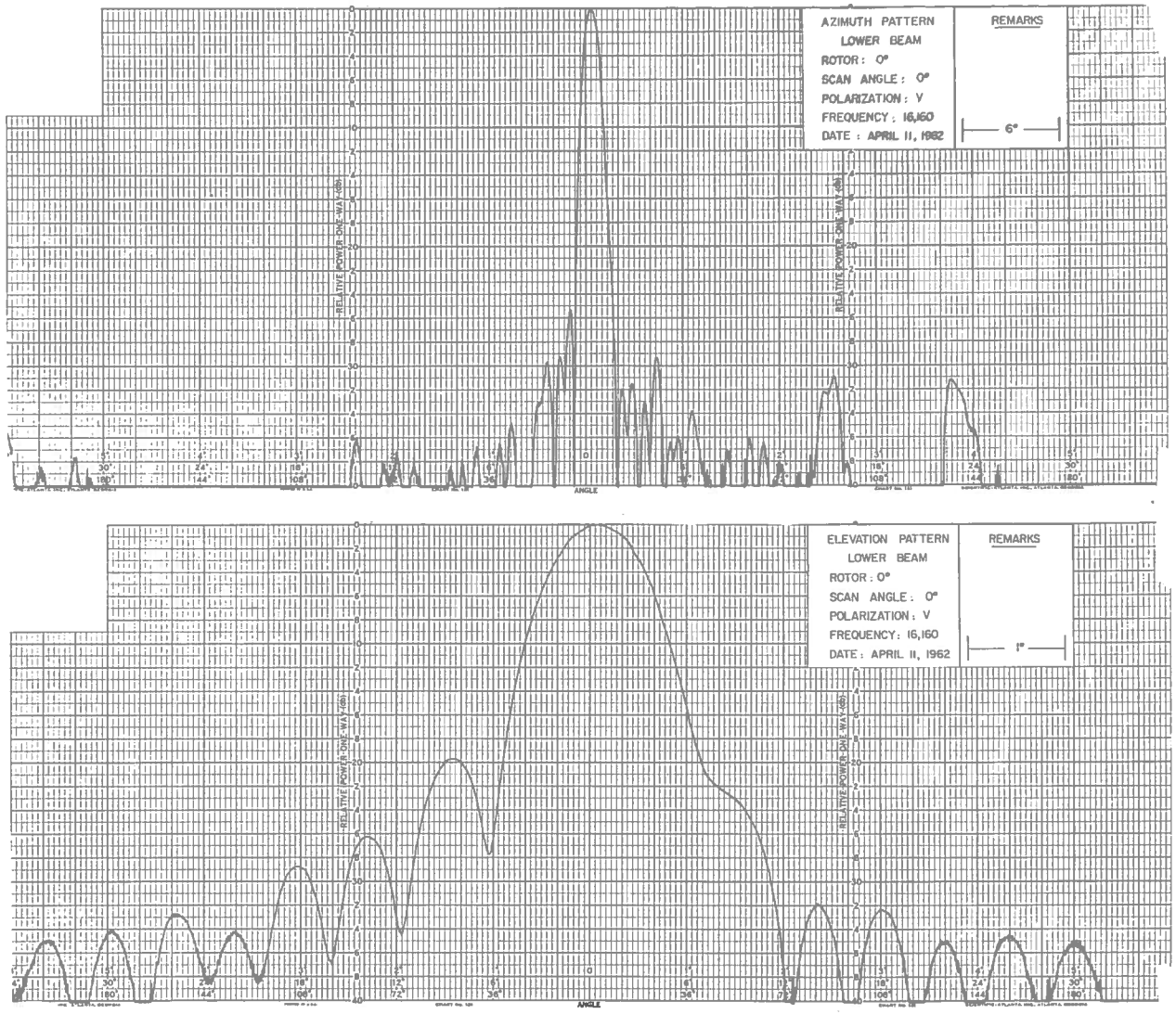

Fig. 18 Radiation patterns. $f = 16{,}160$ mc/s. Rotor = 0°. (before roading)

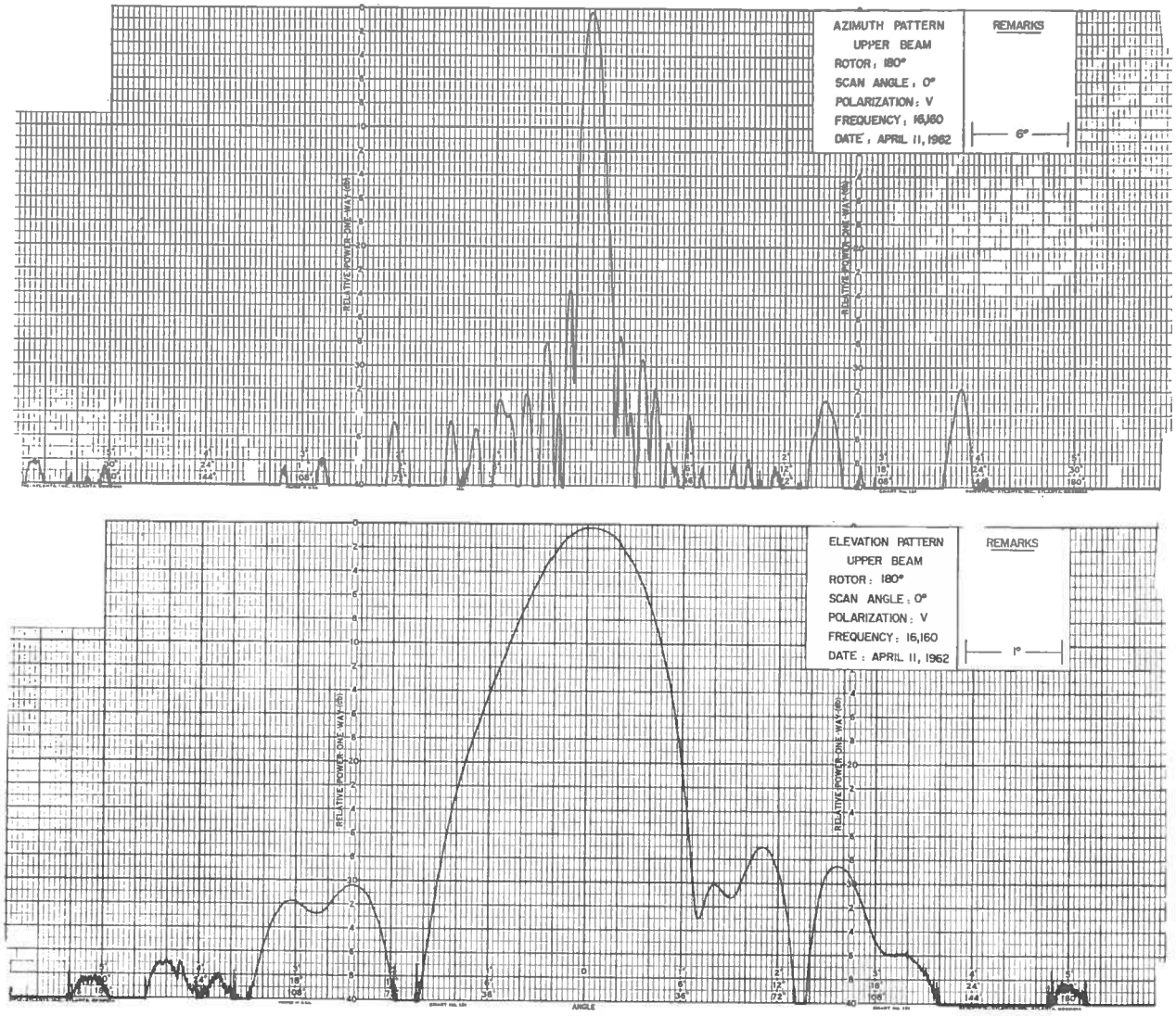

Fig. 19 Radiation patterns. $f = 16{,}160$ mc/s. Rotor = 180°. (before roading)

ii) Side Lobes : Azimuth

a) Lower Beam The first side lobe toward the load end was approximately -21 db at 15,840 mc/s, and in the order of -21 db to -25 db at the other two frequencies. The corresponding value for the feed side was -26 db to -30 db at the three frequencies.

b) Upper Beam This was not significantly different from lower beam.

iii) Wide-angle Lobes (These will be classified according to their origin.)

a) Second-order Beams These arise owing to an asymmetry of odd-numbered slots versus even-numbered slots, and occur at 36° toward the feed end. A maximum amplitude of -30 db was observed at 16,160 mc/s at rotor scale 80.

b) Termination Lobe A lobe occurs at 22° toward the feed end owing to reflection from the slotted array termination. A maximum lobe of -30 db was observed, corresponding to a termination VSWR of 1.3.

c) Slot Grouping The milling of slot offsets in groups of five should result in a small double lobe centered about 14.5° toward the feed end. Such was observed, although considerably distorted, on practically every azimuth pattern, with a maximum amplitude of -30 db.

d) Miscellaneous Lobes Lobes of -30 db or lower can be expected from a slotted array with a number of slots out of tolerance. No evidence of such was observed.

e) Internal Reflection Lobes These lobes arise owing to reflections at the internal bends or at the horn mouth. The slotted array functions like a mirror to this reflected radiation, with the result that it is radiated at an angle from the main beam depending on scan angle. One order of lobes occurs at $(22 + 2\theta)$ degrees from the main lobe, where θ is the scan angle (all angles considered positive toward the feed end), and a second-order lobe occurs at $(44 + 2\theta)$ degrees. A first-order lobe as high as -19 db was observed, and a second-order lobe as high as -23 db. The reflection lobes will be noted in Figs. 20 and 21.

After roading, a few minor changes in side-lobe structure were observed. The side lobe over the lower beam was reduced in magnitude by an average of 1.5 db. Reflection lobes were altered in that maximum amplitudes occurred at different rotor settings. A slight mechanical shift within the scanner could account for the latter effect. No certain explanation for the reduction in the elevation side lobe has been found.

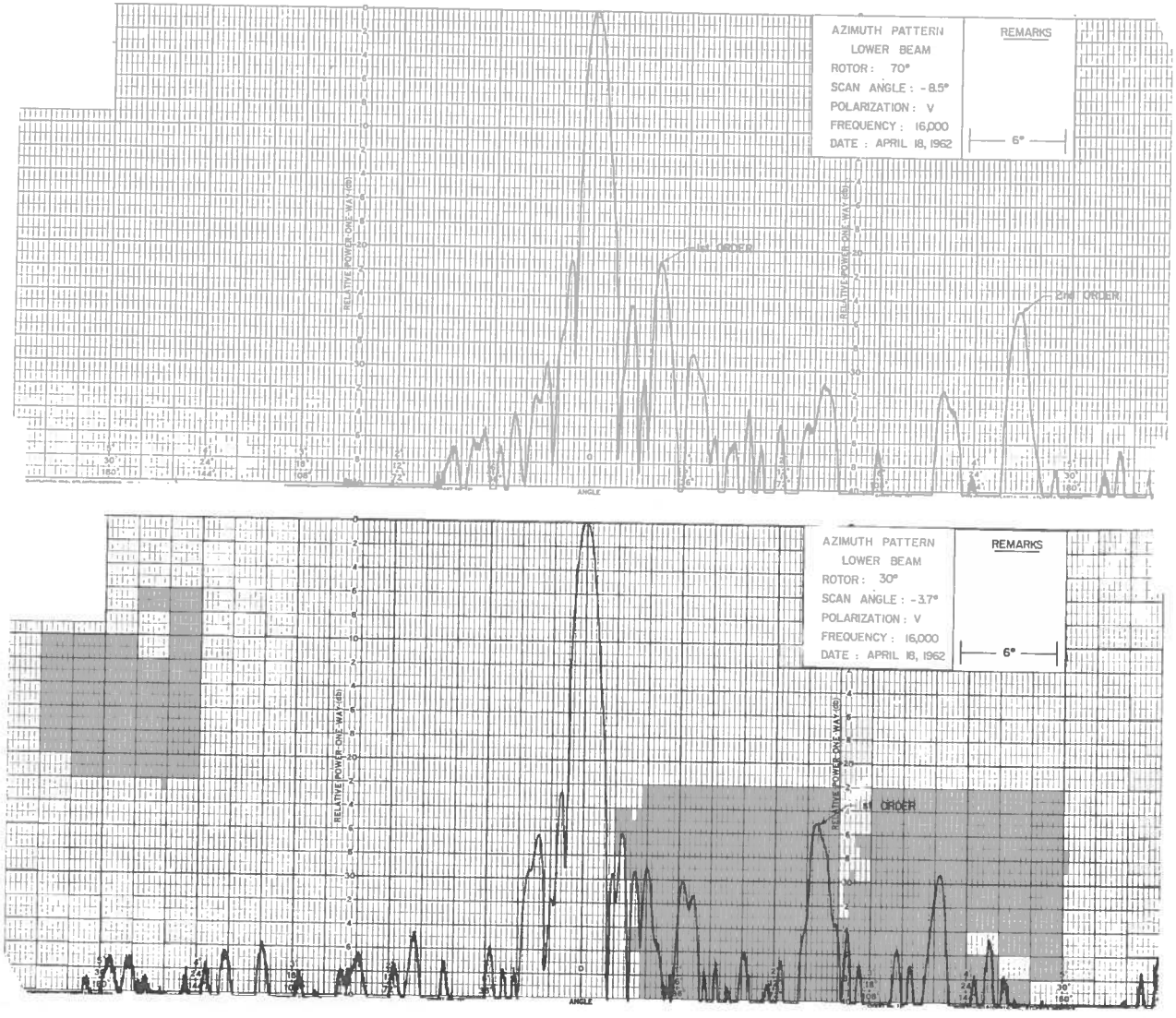

Fig. 20 Radiation patterns. $f = 16,000$ mc/s. Rotor = 70° and rotor = 30°. (Note occurrence of first order and second order reflection lobes.) (before roading)

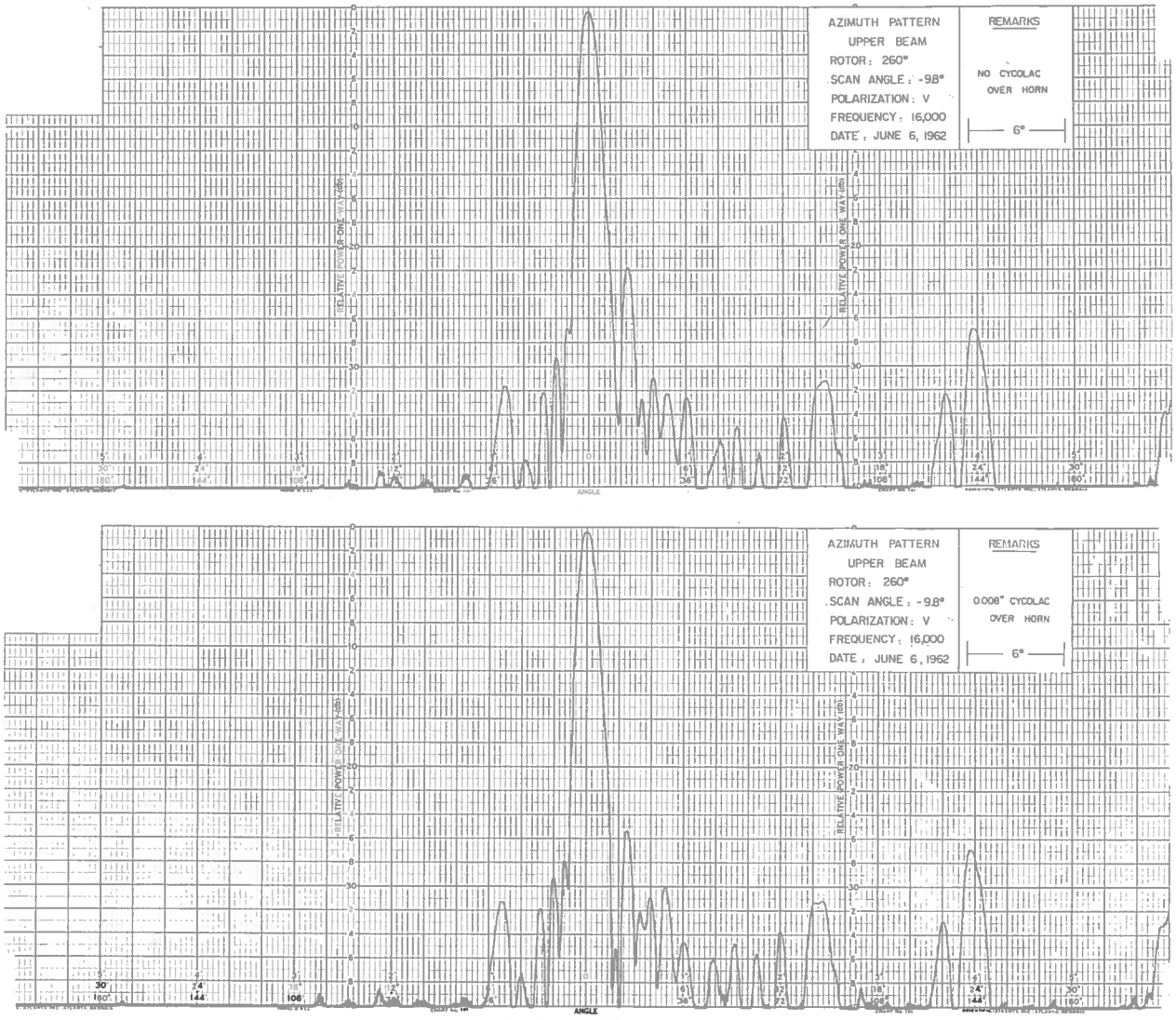

Fig. 21 Radiation patterns. $f = 16,000$ mc/s. Rotor = 260°. (Note change in the first order reflection lobe due to the presence of Cycolac sheet.) (after roading)

Beamwidths

Beamwidth determinations were obtained with a theodolite incidental to the determination of beam position. These measurements are more accurate than those obtained with the decibel recorder. Beamwidths are shown in Table I(a) and Table I(b).

Effect of Absorbing Materials on Side Lobes

Earlier work on elevation patterns using a 1-foot test section indicated that there was some possibility of the occurrence of -26 db side lobes under lower beam, and in addition, that these could be reduced to negligible magnitude by the placement of microwave absorber on the exterior of the horn cover. The horn cover, was consequently, made with a protruding lip to accommodate the absorber, if necessary. It has been found that the side lobe in question is less than -30 db, and therefore that the absorber is not required. There is no reason why the lip cannot be removed, leaving a cover of circular cross section as shown in the horn assembly, Fig. 48.

The effect of absorbing materials when attached to the machined right-angled surface connecting the two horns was tried. The use of a $\frac{1}{8}$-inch flexible absorber (Emerson and Cuming LS-22) produced a reduction of 2 db in the side lobe immediately over the lower beam. No adverse effect on gain or any other antenna characteristic was noted. The use of this or a similar absorber is, therefore, tentatively recommended. Representative patterns with, and without the absorber are shown in Figs. 22 to 24.

Effects of Reflector Contour and Elevation Geometry

The reflector contour and the positioning of the reflector with respect to the horns were checked after roading. Some small changes had apparently occurred; however, only a few small areas showed contour errors in excess of 0.030 inch, and the quality of the reflector was still high. It is estimated on the basis of previous experience that elevation side lobes at the 25 db level might have been affected to the extent of 1 db by changes in reflector contour.

Any excess motion of the actuator which raises the reflector is taken up in a spring. With the original spring and without the use of the actuator microswitch, uncertainty existed in the positioning of the reflector with respect to the horns. When the horn cover was removed and the focal line of the reflector located with a template, it was found that it was displaced 0.050 inch to 0.090 inch from its correct position with the reflector erected in the usual manner. Many patterns were taken with this geometry. However, no great change in the

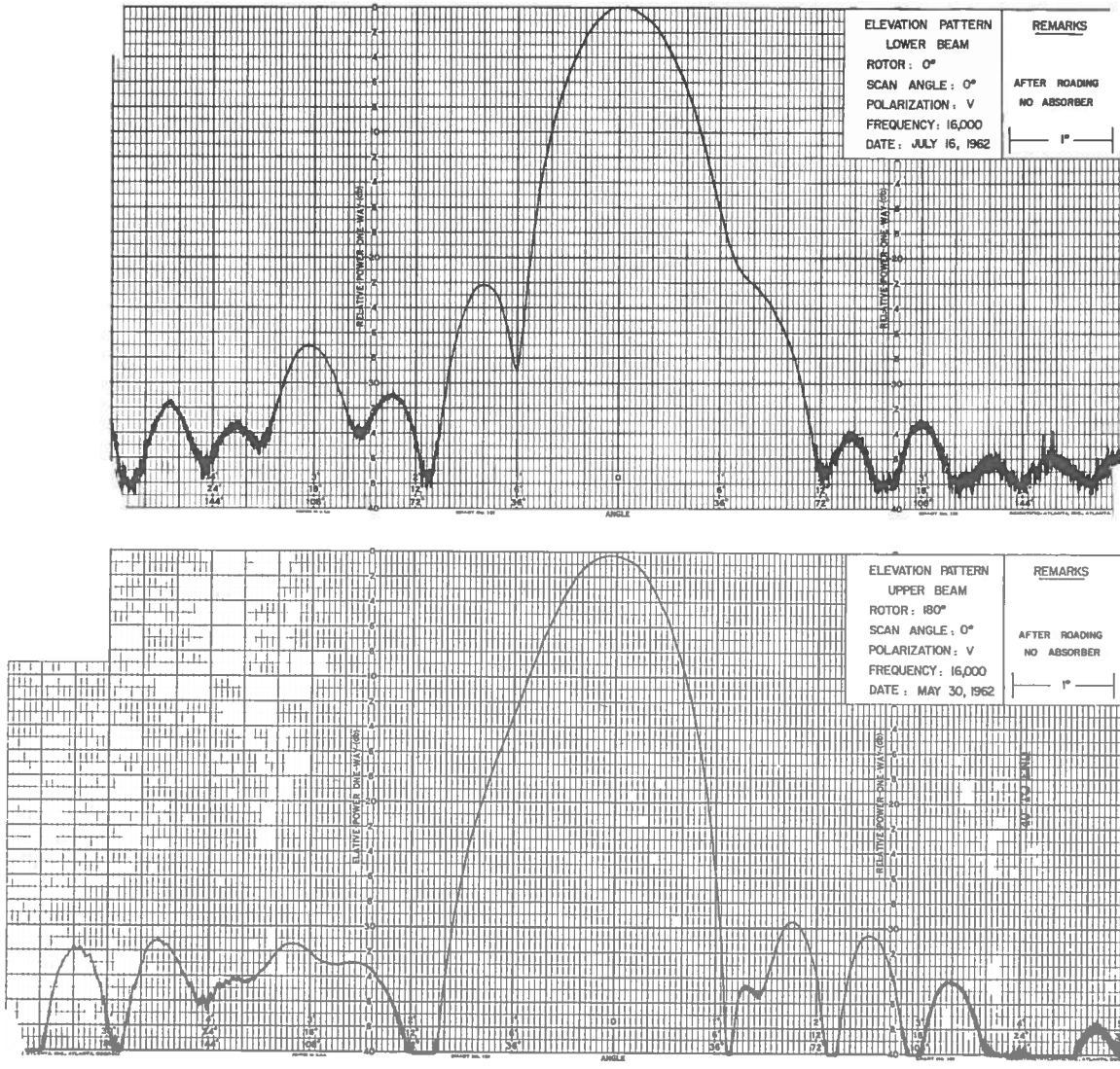

Fig. 22 Radiation patterns in elevation. Scan angle = 0°, $f = 16,000$ mc/s
Upper and lower beams. (without LS-22 absorber)

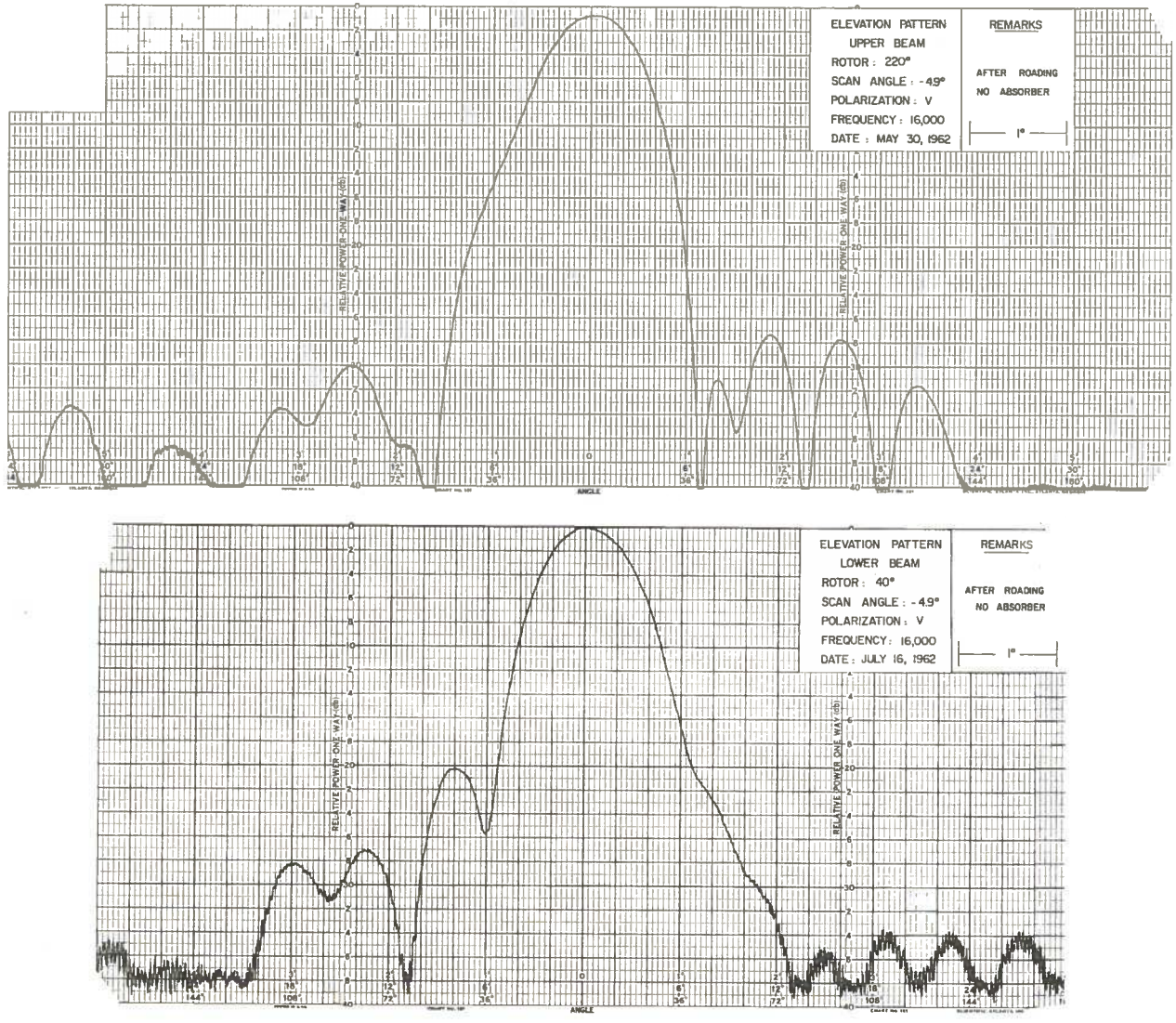

Fig. 23 Radiation patterns in elevation. Scan angle = -4.9°
Upper and lower beams. (without LS-22 absorber)

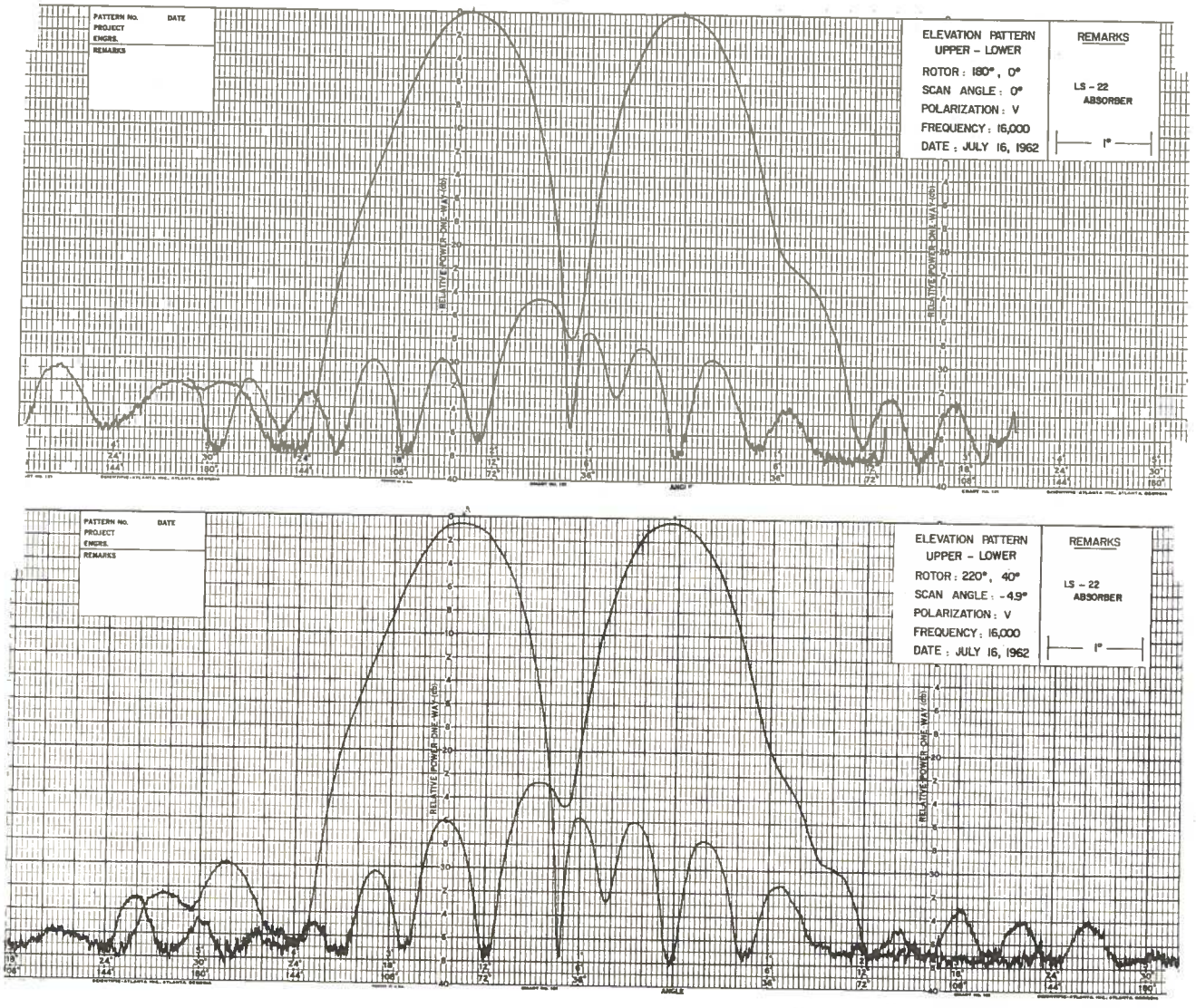

Fig. 24 Radiation patterns in elevation. Scan angles = 0° and -4.9°
Upper and lower beams. (with LS-22 absorber)

TABLE I(a)

AZIMUTH BEAMWIDTHS

	Frequency (mc/s)	Beamwidth (degrees)		Frequency (mc/s)	Beamwidth (degrees)
Lower beam	15,840	0.85	Upper beam	15,840	0.85
Lower beam	16,000	0.86	Upper beam	16,000	0.85
Lower beam	16,160	0.86	Upper beam	16,160	0.86

TABLE I(b)

ELEVATION BEAMWIDTHS

Rotor Lower Beam	Frequency (mc/s)	Beamwidth (degrees)	Rotor Upper Beam	Frequency (mc/s)	Beamwidth (degrees)
280	15,840	0.83	100	15,840	0.84
320	"	0.86	140	"	0.87
0	"	0.82	180	"	0.87
40	"	0.84	220	"	0.86
80	"	0.82	260	"	0.83
280	16,000	0.83	100	16,000	0.84
320	"	0.84	140	"	0.86
0	"	0.82	180	"	0.85
40	"	0.85	220	"	0.85
80	"	0.84	260	"	0.84
280	16,160	0.84	100	16,160	0.84
320	"	0.83	140	"	0.88
0	"	0.84	180	"	0.87
40	"	0.84	220	"	0.86
80	"	0.82	260	"	0.85

elevation patterns takes place when the reflector position is changed to optimum: the side lobe over the lower beam is decreased by 0.8 db, and there is a similar increase in the side lobe immediately under the upper beam.

Effect of a Horn Matching Technique

It was noted above that reflection within the scanner and at the horn mouth gave rise to wide-angle radiation that produced lobes which in a few instances exceeded -20 db. It was known that some mismatch (VSWR =1.08) existed in the horn which produces the upper beam, and furthermore, that it could be matched by means of one layer of 0.008 inch Cycolac sheet attached across the horn mouth. The use of this Cycolac sheet on the scanner horn produced a 4 db improvement in the lobe in question (Fig. 21). Its use in production units is recommended. A similar, although smaller improvement is possible on the lower beam by the use of a 0.005 inch Teflon tape over the horn mouth.

GAIN

Received signals were taken simultaneously from the scanner and from a standard gain horn, and an amplitude comparison was made. The reading of a precision microwave attenuator used for balancing the circuit gave the relative gains of the two antennas when corrections were made for the insertion loss.*

---

* Two other minor corrections were necessary. First, in spite of the use of diffraction screens, ground reflections produced a measurable effect on the signal received by the standard gain horn, particularly the smaller one used for the earlier measurements. The correction was determined by readings obtained while raising and lowering the horn and associated equipment. The maximum correction was 0.13 db for the smaller horn and 0.08 db for the larger. Secondly, the separation of the scanner and the horn had to be taken into account. It was found that accurate gain measurement could be obtained only if the transmitting antenna was carefully peaked on the scanner at rotor setting zero. The signal from the transmitting paraboloid was 0.44 db down at the position of the horn, which was at a distance of 8 feet. This is in agreement with the measured pattern of the five-foot paraboloid. Consequently, a correction of -0.44 db was applied to measured gain values. There was some apprehension concerning the proximity of the horn to the scanner; however, careful tests showed that there was no significant interaction.

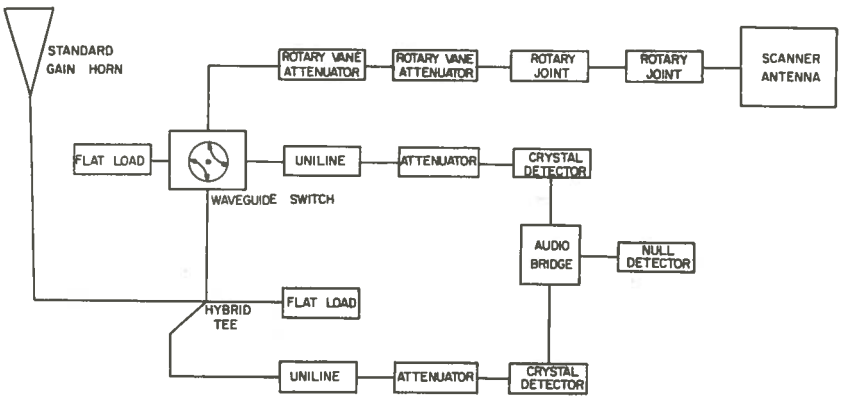

Fig. 25 Block diagram of apparatus for the measurement of gain

Figure 25 is a block diagram of the gain measurement apparatus. Insertion losses were obtained by a standard method for the measurement of scattering coefficients. Initially, the various parts were measured separately. As a final check, measurements for the complete horn line and the complete scanner line were made in situ. For measurements before roading, a standard gain horn of

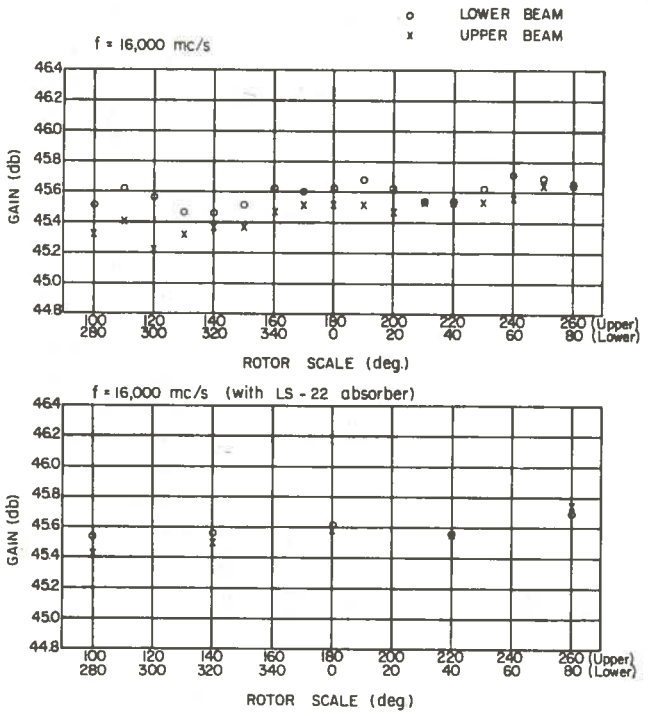

Fig. 29 Gain of antenna at 16,000 mc/s, with and without LS-22 absorber. (after roading)

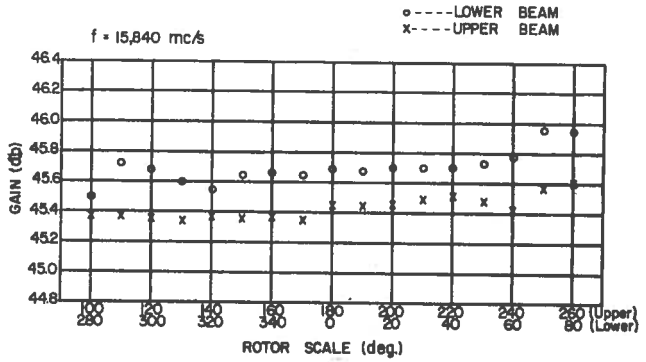

Fig. 26 Gain of antenna at 15,480 mc/s. (before roading)

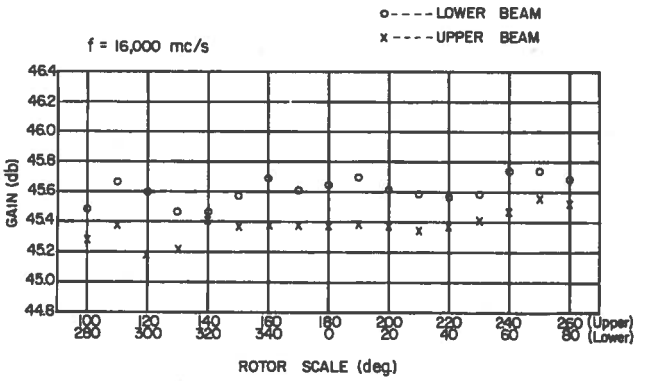

Fig. 27 Gain of antenna at 16,000 mc/s. (before roading)

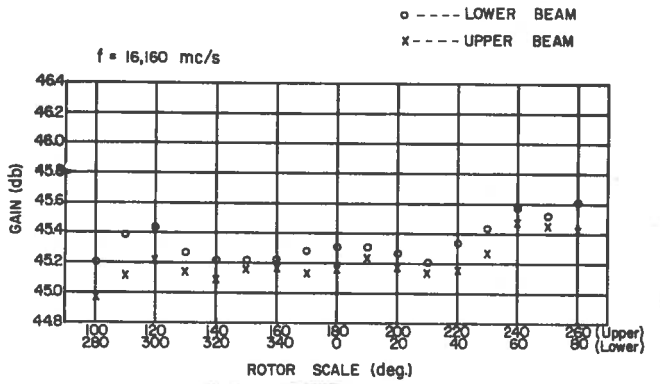

Fig. 28 Gain of antenna at 16,160 mc/s. (before roading)

familiar design [8] was used, having a calculated gain of 24.68 db at 16,000 mc/s. For measurements obtained after roading, a larger optimum gain horn having a calculated gain of 29.54 db at 16,000 mc/s was used. The estimated error in the measurement of the gain is ±0.2 db.

The gain is shown plotted as a function of rotor setting for various frequencies and conditions, in Figs. 26 to 29. It will be noted that roading caused no deterioration in gain. 45.0 db is a conservative figure for the gain of the antenna.

Calculations were made from azimuth and elevation field strength patterns taken at 16,000 mc/s in order to find the directive gain of the antenna. Antenna losses at 16,000 mc/s which were calculated mainly on the basis of measured quantities, are tabulated in Table II, and are believed accurate within the limits shown.

TABLE II

ANTENNA DIRECTIVITY AND LOSSES AT 16,000 MC/S

Directive gain at center of scan		46.90 ±0.15 db
Losses in:		
a) internal waveguide and rotating joint	0.20 ±0.05 db	
b) slotted array	0.18 ±0.05 db	
c) slotted array termination	0.18 ±0.02 db	
d) reflector spillover	0.10 ±0.05 db	
e) internal surface losses (based on a measured skin depth of 2.5×10^{-4} cm)	0.77 ±0.10 db	
Total losses		1.43 ±0.13 db
Calculated power gain		45.47 ±0.20 db

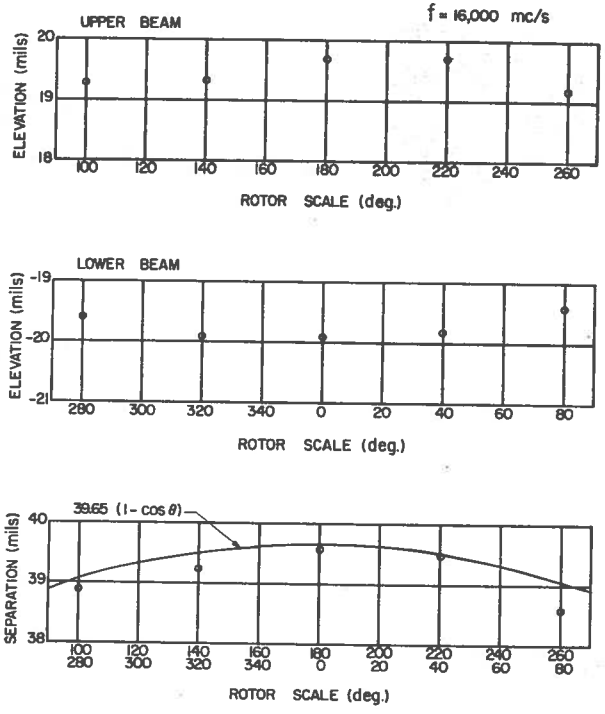

Fig. 30 Beam elevation and beam separation at 16,000 mc/s (referred to a plane parallel to the rocker arm pad). (before roading)

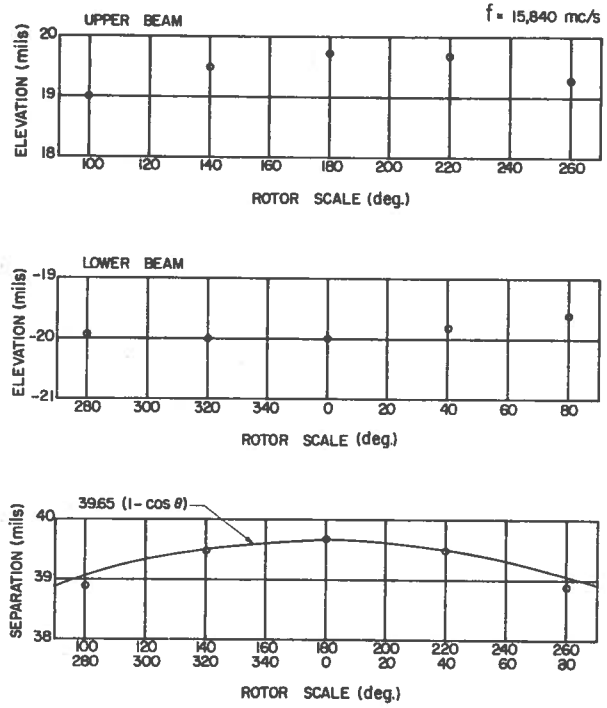

Fig. 31 Beam elevation and beam separation at 15,840 mc/s (referred to a plane parallel to the rocker arm pad). (after roading)

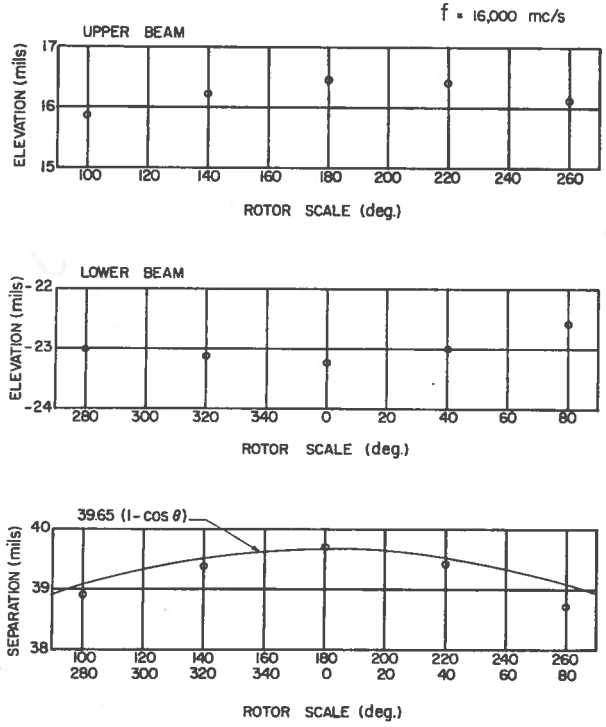

Fig. 32 Beam elevation and beam separation at 16,000 mc/s (referred to a plane parallel to the rocker arm pad). Reflector re-positioned for optimum focus. (after roading)

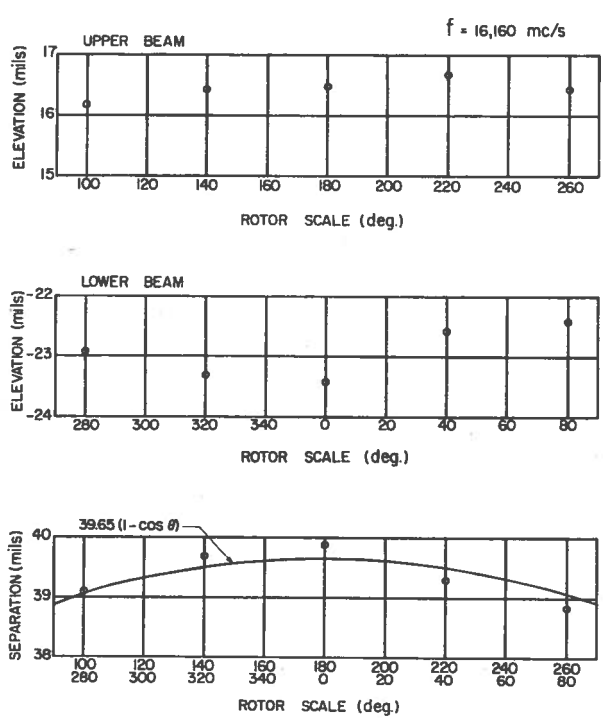

Fig. 33 Beam elevation and beam separation at 16,160 mc/s (referred to a plane parallel to the rocker arm pad). Reflector re-positioned for optimum focus. (after roading)

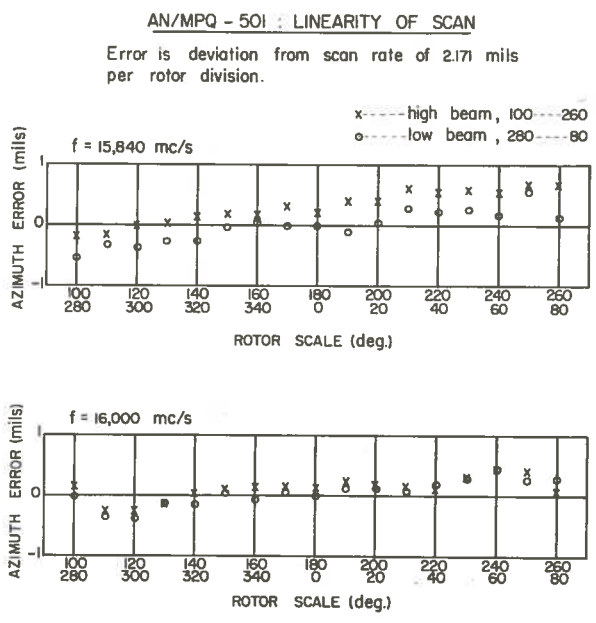

NOTE : Separation of high beam points and low beam points gives azimuth beam separations for corresponding rotor positions. Positive error means a beam displacement toward the load end.

Fig. 34 Error in linearity of scan before road tests (error set arbitrarily at zero for rotor zero)

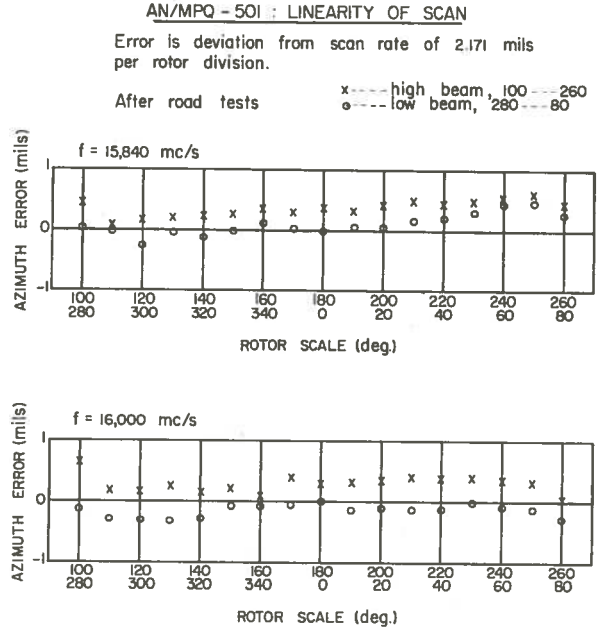

Fig. 35 Error in linearity of scan, after road tests (error set arbitrarily at zero for rotor zero)

BEAM POSITION

Measurements of beam position included: (1) the location of the beam in elevation with respect to a fixed reference, (2) the angle of separation of the two beams, (3) the change in azimuth scan angle with rotor position, (4) the change of scan angle with frequency. Most of the beam position measurements were made with a Wild theodolite specially mounted at the base of the reflector. The assessment of the optimum limits of scan, which is dealt with in the next section, was made on the basis of radiation patterns. Over a range of reasonable length it is necessary to make corrections for the displacement of the optical axis from the electrical axis. The location of the phase center upon which this correction depends is discussed in a subsequent section.

Elevation Beam Position

The reference for the location of beams in elevation is a machined pad on the rocket arm near the large end of the scanner. Elevations are recorded with respect to a plane parallel to the rocket arm pad. Variations in actuator extension against the take-up spring produced a change in beam elevation of over one-third of a degree. Special means were employed by use of the theodolite level and the levelling of the pad to obtain a definite setting. Beam elevations as a function of rotor position are given in Figs. 30 to 33. These points are corrected for axis displacement. Beam separations are shown on the same figures. The solid curve indicates the theoretical separation as a function of scan angle about two planes of dihedral angle 2° 14'.

Linearity of Scan

The error in azimuth beam position is shown plotted in Figs. 34 and 35. The error is arbitrarily set equal to zero at rotor setting zero, and is the deviation

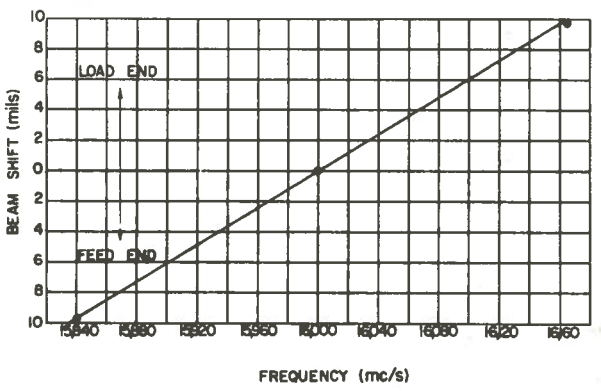

Fig. 36 Beam shift versus frequency shift

in beam position from the ideal position based on the theoretical scan rate of 2.171 mils per rotor degree. These points have been corrected for the variation in the location of the phase center.

Scan Angle versus Frequency

The variation of scan angle with frequency is directly related to the frequency dependence of the squint angle of the slotted array. Scan angle versus frequency is shown plotted in Fig. 36.

OPTIMUM CENTER OF SCAN

Patterns were taken at closely spaced rotor intervals near the limits of scan on each beam. In this way, the onset of deterioration with approach toward the switch region was noted. The limits of scan, chosen to give the best 20° of azimuth scan, are shown in Table III. It should be noted that the rotor scale indication of scan limits is independent of frequency*. The inclination to normal will, of course, vary with frequency.

TABLE III

LIMITS OF SCAN

	Rotor Scale	Inclination to Normal at 16,000 mc/s
Lower beam, left	87°	-10.71°
Lower beam, center	4°	- 0.61°
Lower beam, right	281°	+ 9.51°
Upper beam, left	267°	-10.71°
Upper beam, center	184°	- 0.61°
Upper beam, right	101°	+ 9.51°

PHASE CENTER OF THE SCANNER

Any tests or checks of beam position made at short range — say, 600 to 4000

* It is probable that the positioning of the rotor scale relative to the switch region will be closely reproduced in the manufacture of each of the series of antennas. However, for test purposes, and for reference, some means for the permanently accurate and reproducible reading of the scale should be provided.

feet — require corrections for phase center location. Consequently, apparatus was developed for the accurate location of the phase center. The device consists of two pairs of horns, one for elevation and the other for azimuth, each pair being connected to a hybrid so that a null results when the axis of the device passes through the phase center [7]. A photograph is shown in Plate II.

The results obtained on the Serial 1 production set for lower beam at 16,000 mc/s were:

Elevation position — 28.0 inches ±0.5 inch vertically above base of reflector. (This equals 29.3 inches above the base of the reflector as measured on the reflector.)

Azimuth position (Boresight at -0.6° to normal.) — 0.6 inch ±0.5 inch from center of reflector toward large end of scanner.

The variation of these positions with frequency can be expected to be less than one inch. A theoretical curve for the variation of phase center location with scan angle is shown in Fig. 37.

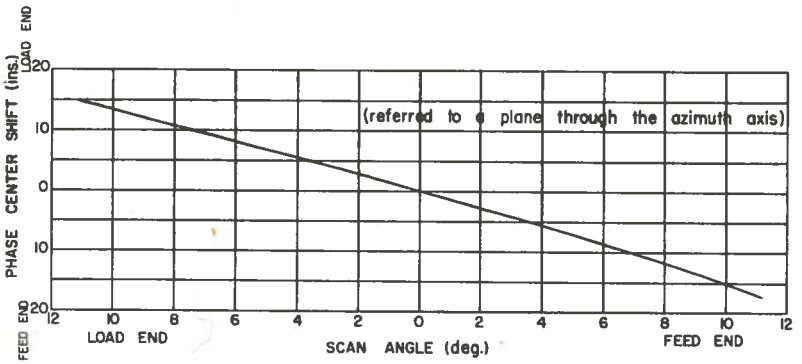

Fig. 37 Phase center shift versus scan angle

It should be noted that the phase center, which can be obtained directly in a straightforward manner, is not necessarily the intersection in the aperture of the straight line drawn through the peak of the beam at various distances in the far field. This is because of asymmetry of the field in the aperture. However, for lower beam on the scanner, calculation shows that these points are separated by less than one-half inch.

POLARIZER TESTS

Representative rectangular patterns were taken with the production polarizer in place, several of which are reproduced in Figs. 38 to 41. The azimuth patterns are changed only in minor details from the corresponding patterns without the polarizer. More significant changes will be noted in the elevation patterns.

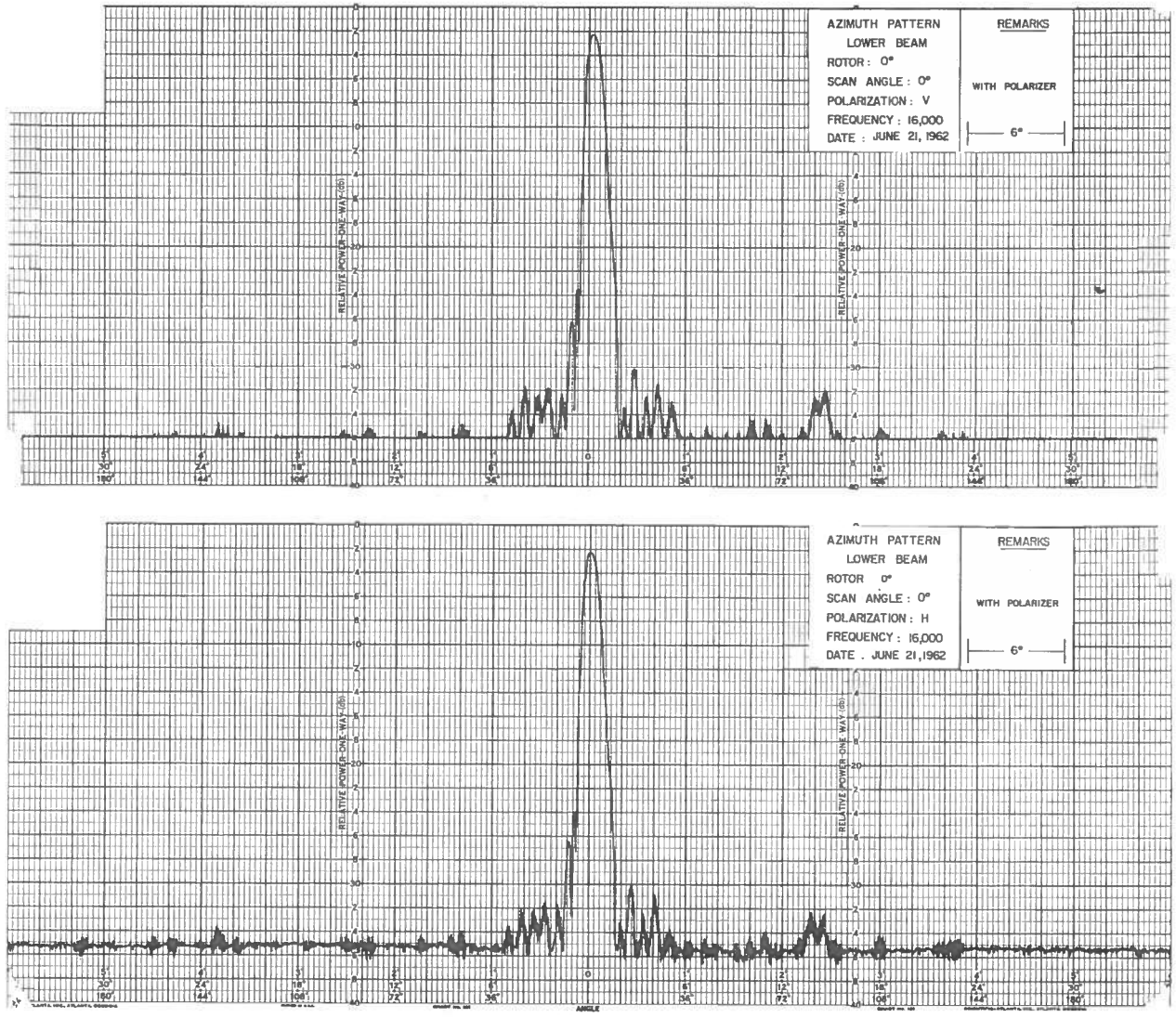

Fig. 38 Azimuth patterns with polarizer. Transmitter vertically and horizontally polarized. Rotor = 0°, $f = 16,000$ mc/s

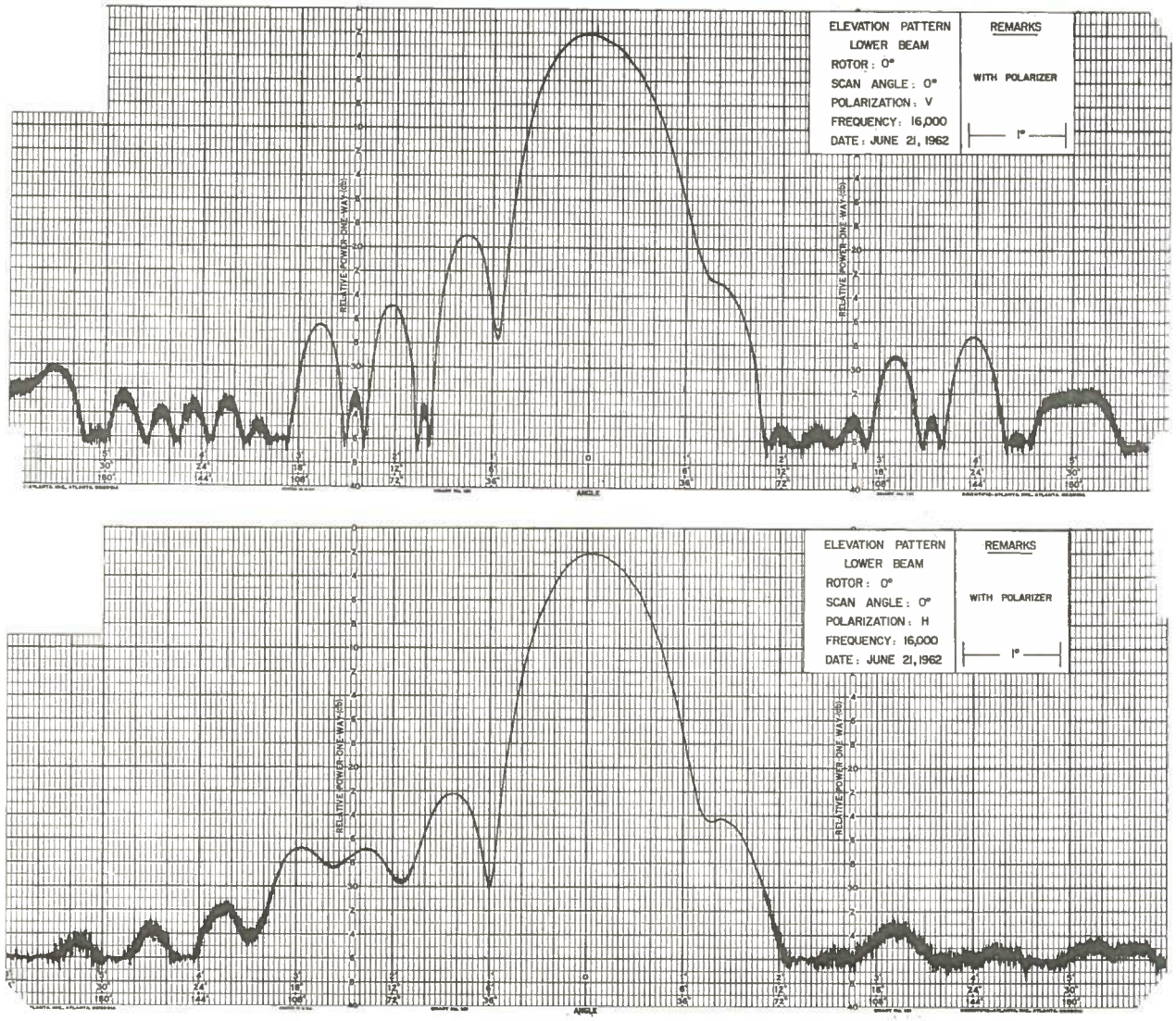

CONFIDENTIAL

Fig. 39 Elevation patterns with polarizer. Transmitter vertically and horizontally polarized. Rotor = 0°, $f = 16,000$ mc/s

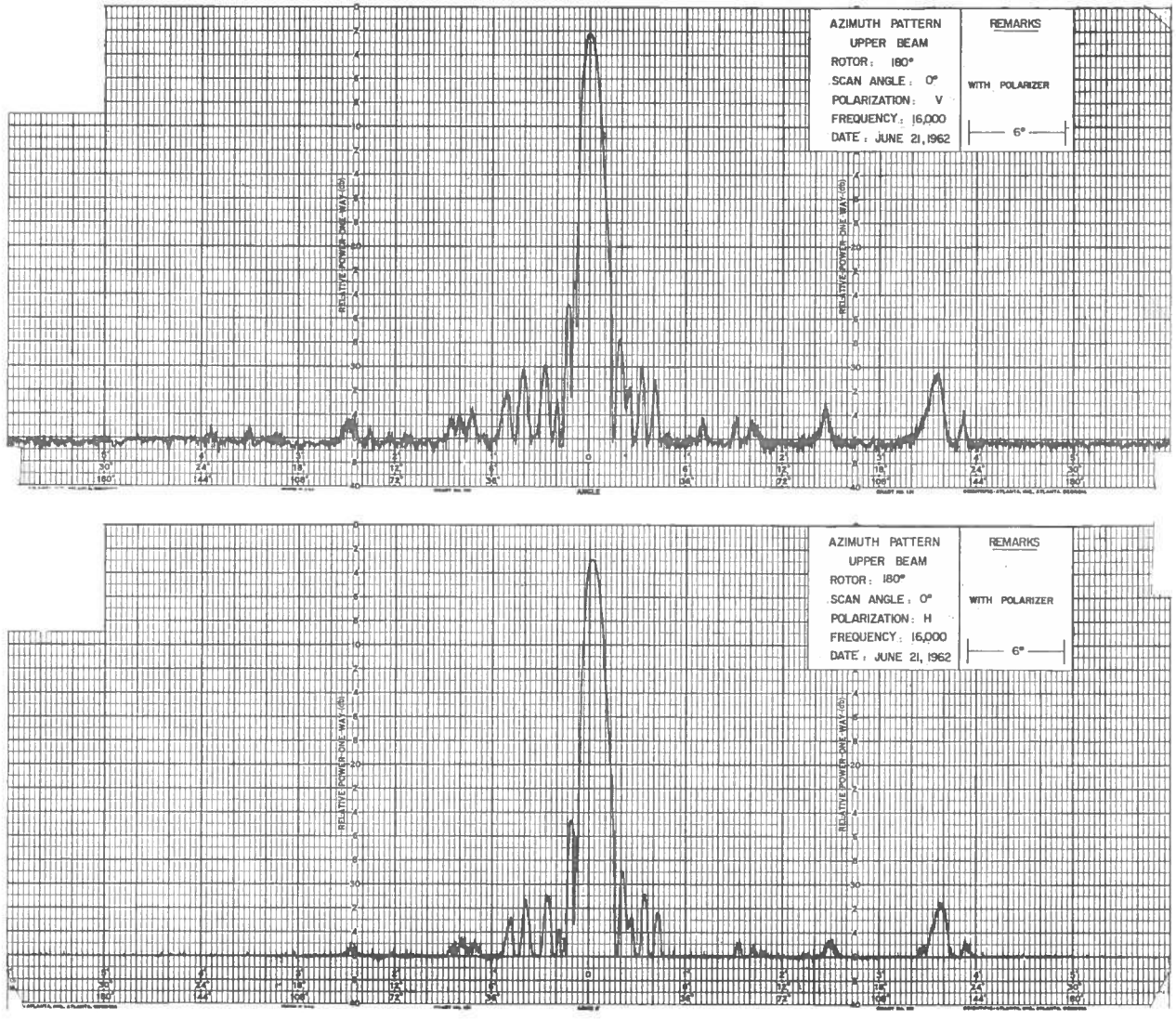

Fig. 40 Azimuth patterns with polarizer. Transmitter vertically and horizontally polarized. Rotor = 180°, $f = 16,000$ mc/s

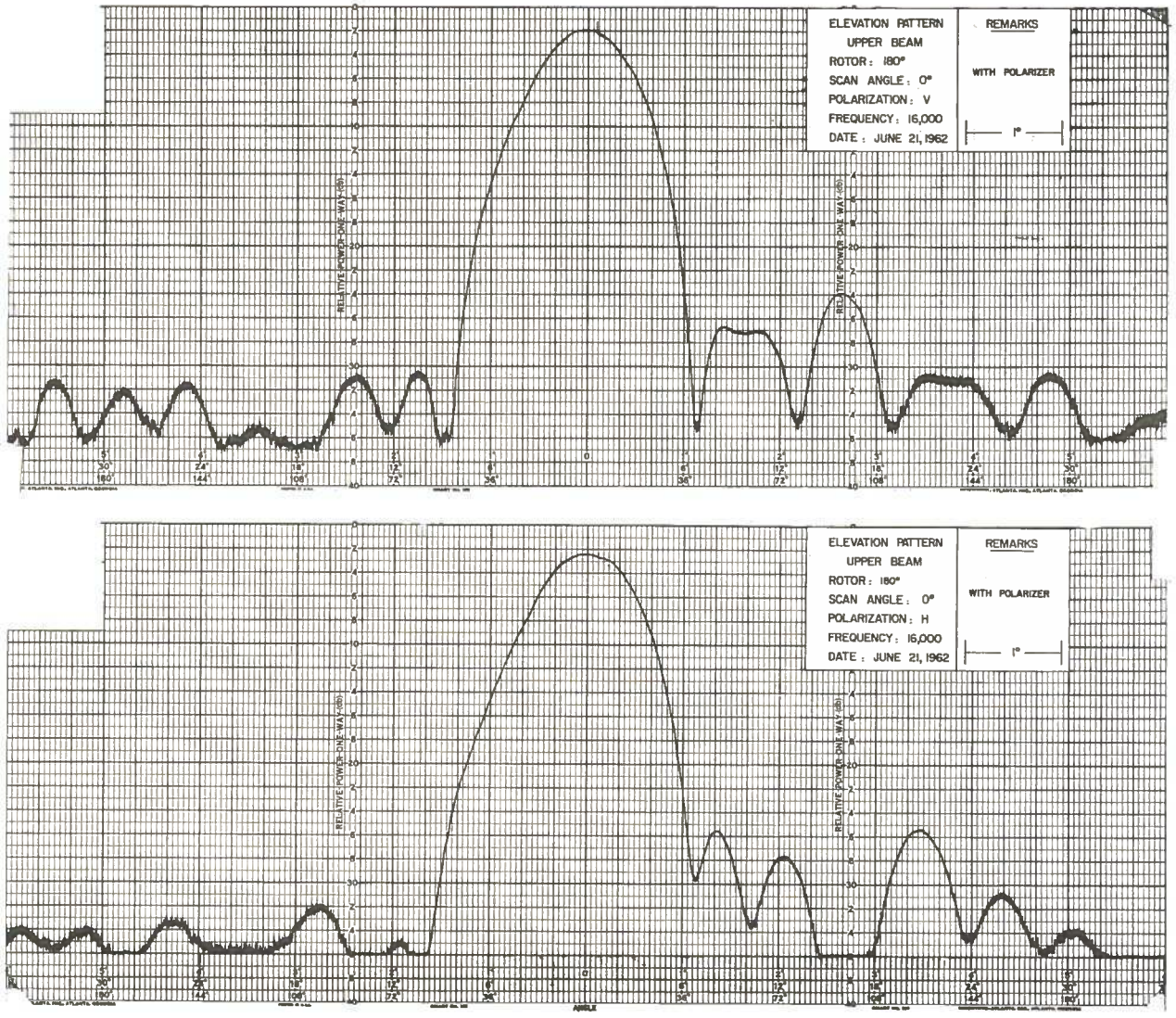

Fig. 41 Elevation patterns with polarizer. Transmitter vertically and horizontally polarized. Rotor = 180°, $f = 16,000$ mc/s

The side lobe over lower beam has at some rotor settings increased to -17 db, and the beamwidth exhibits a greater variation with rotor setting than was anticipated.

Beamwidth and beam position were checked with the theodolite. Typical beamwidths and corresponding beam separation are shown in Table IV. The linearity of scan was checked on upper beam for each polarization, i.e., transmission with vertical or horizontal polarization, and found to be only slightly inferior to data obtained without the polarizer.

TABLE IV

ELEVATION BEAMWIDTHS WITH POLARIZER (f = 16,000 mc/s)

Rotor (lower beam)	Beamwidth (degrees)	Rotor (upper beam)	Beamwidth (degrees)	Beam Separation (mils)
a) Vertical Polarization				
280	0.83	100	0.84	38.8
320	0.85	140	0.88	39.0
0	0.88	180	0.90	39.3
40	0.83	220	0.87	38.8
80	0.82	260	0.85	38.1
b) Horizontal Polarization				
280	0.84	100	0.87	38.7
320	0.86	140	0.91	39.0
0	0.88	180	0.92	39.1
40	0.87	220	0.90	39.2
80	0.83	260	0.87	39.1

Since elevation beamwidth variation with the polarizer amounts to a total of 7% on lower beam and 6% on upper beam, it should be noted that without the polarizer there is a 4% variation with scan angle on lower beam. This latter variation is apparently due to scattering by the feed assembly of the secondary radiation from the reflector. Owing to its size, the polarizer may increase this scattering, and may scatter the upper beam as well as the lower; in addition, the effectiveness of the polarizer depends on the angle of incidence which, in turn, can lead to a variation with scan angle.

A comparison of Table IV with Figs. 30 and 32 will show the extent of change in beam separation produced by the polarizer. The lower beam was raised 0.8 mil on vertical polarization and 0.5 mil on horizontal polarization owing to the presence of the polarizer. The corresponding figures for the upper beam are 0.2 mil and 0.1 mil. In brief, beam separation has been decreased one-half mil owing to the raising of the lower beam.

Values of the gain of the antenna measured directly with the polarizer in place are shown in Table V. The total for the two components is shown for comparison with the values previously measured using linear polarization. The comparison is consistent with a theoretical loss in the polarizer of 0.2 db based on a loss tangent for Cycolac of 0.005.

TABLE V

ANTENNA GAIN WITH POLARIZER (f = 16,000 mc/s)

Rotor	Gain (db) Xmtr. : vert. Rcvr. : circ.	Gain (db) Xmtr. : horiz. Rcvr. : circ.	Calculated Gain (db) Xmtr. : circ. Rcvr. : circ.	Gain (db) Xmtr. : vert. Rcvr. : vert. (without polarizer)
a) Lower Beam				
280	42.47	42.21	45.35	45.52
320	42.44	42.22	45.34	45.44
0	42.17	42.27	45.23	45.62
40	42.54	42.48	45.52	45.58
80	42.47	42.78	45.63	45.66
b) Upper Beam				
100	41.97	42.20	45.09	45.33
140	42.07	42.17	45.13	45.37
180	42.14	42.12	45.14	45.52
220	42.37	42.23	45.31	45.54
260	42.64	42.32	45.49	45.70

Initial polarization patterns were taken without artificial drying of the polarizer.

A summary of the data obtained is shown in Fig. 42. Most of the patterns were taken while the polarizer was dried by means of a stream of nitrogen. Data are shown in Figs. 42 and 43 and typical patterns in Figs. 44 and 45. The relation between axial ratio and cancellation ratio is given in Table VI.

TABLE VI

CANCELLATION RATIO VERSUS AXIAL RATIO

Axial Ratio	Cancellation Ratio (db)	Axial Ratio	Cancellation Ratio (db)
0.70	9.32	0.94	24.20
0.75	11.08	0.95	25.84
0.80	13.16	0.96	27.80
0.85	15.88	0.97	30.34
0.90	19.58	0.98	33.88
0.91	20.52	0.985	36.40
0.92	21.60	0.99	39.96
0.93	22.80	0.995	46.20
		0.999	60.0

Polarization patterns were taken by rotating the five-foot paraboloid which was mounted on a commercial polarization mount. There was some difficulty with both the proper alignment of the paraboloid and with the operation of the polar recorder. The result is that individual measurements of the axial ratio may be in error by as much as 0.02. However, sufficient data were obtained to provide a reasonable estimate of the limits of error in a number of cases.

It will be noted that the polarizer performance approximates a mean axial ratio of 0.95, which is considerably in excess of the provisional specifications [2]. However, on the basis of previous tests it had been hoped that a value in excess of 0.97 could be maintained over a considerable portion of the scan range. With the need in mind for as high an axial ratio as possible, every practical step was taken to further this end, including the artificial drying of the polarizer. From this point of view the results obtained were disappointing. In fact, the evidence at hand indicates that the performance deteriorated when the polarizer

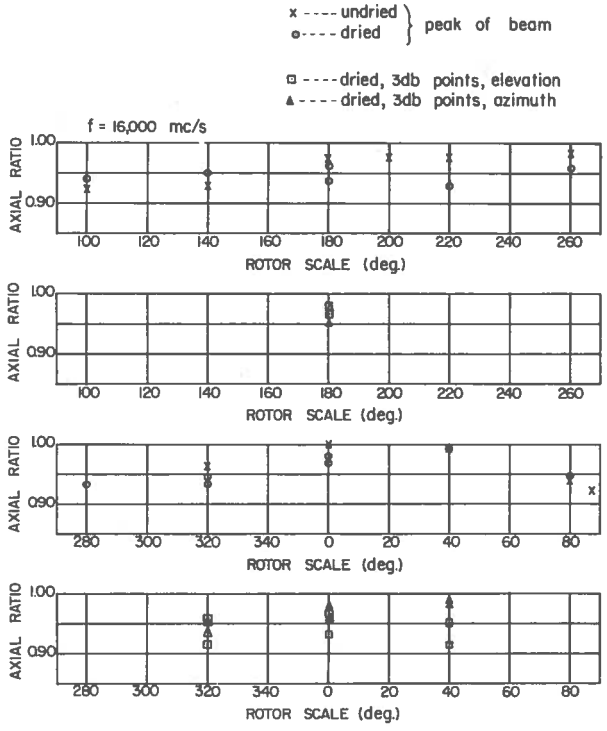

Fig. 42 Axial ratios. $f = 16,000$ mc/s. Data are shown for the peak of the beam and for the 3 db points.

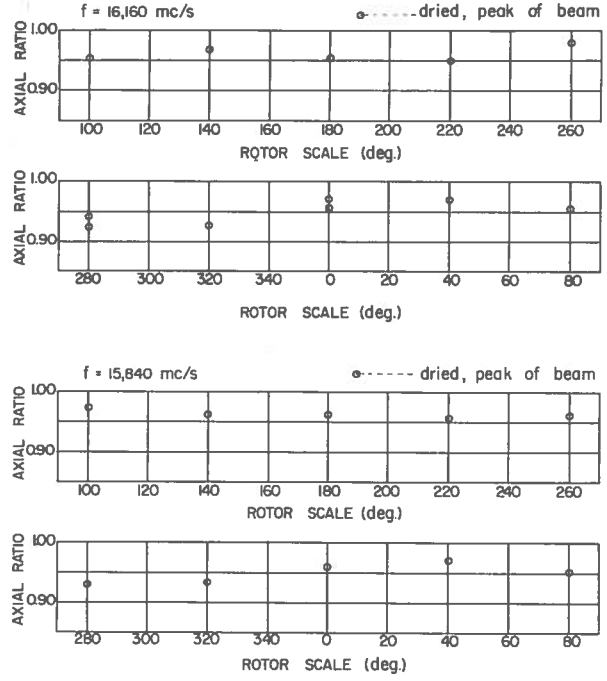

Fig. 43 Axial ratios on the peak of the beam $f = 15,840$ mc/s and 16,160 mc/s

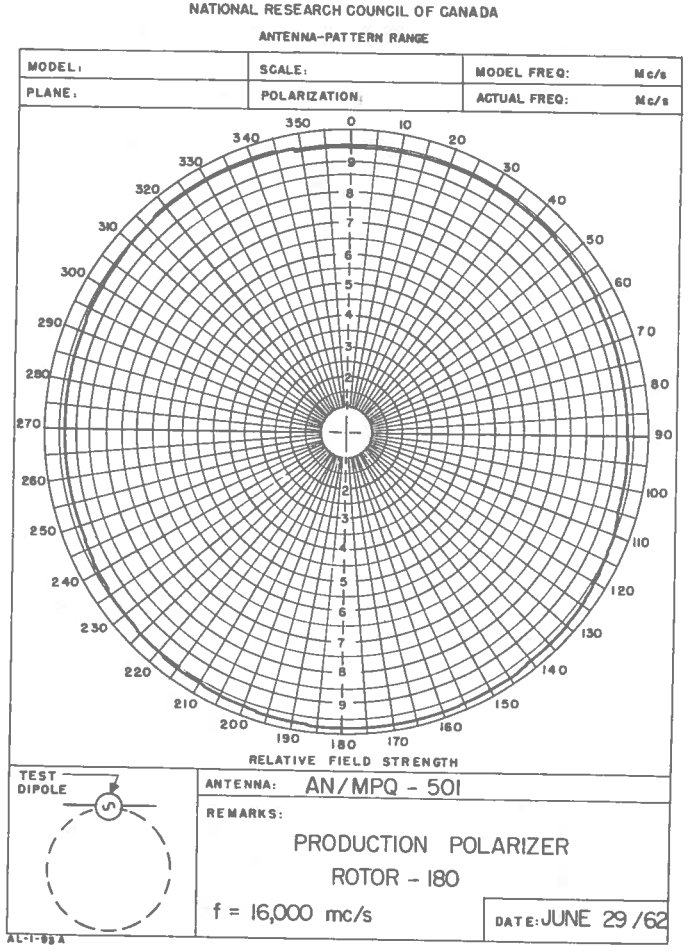

Fig. 44 Polarization pattern. Rotor = 180°, $f = 16,000$ mc/s

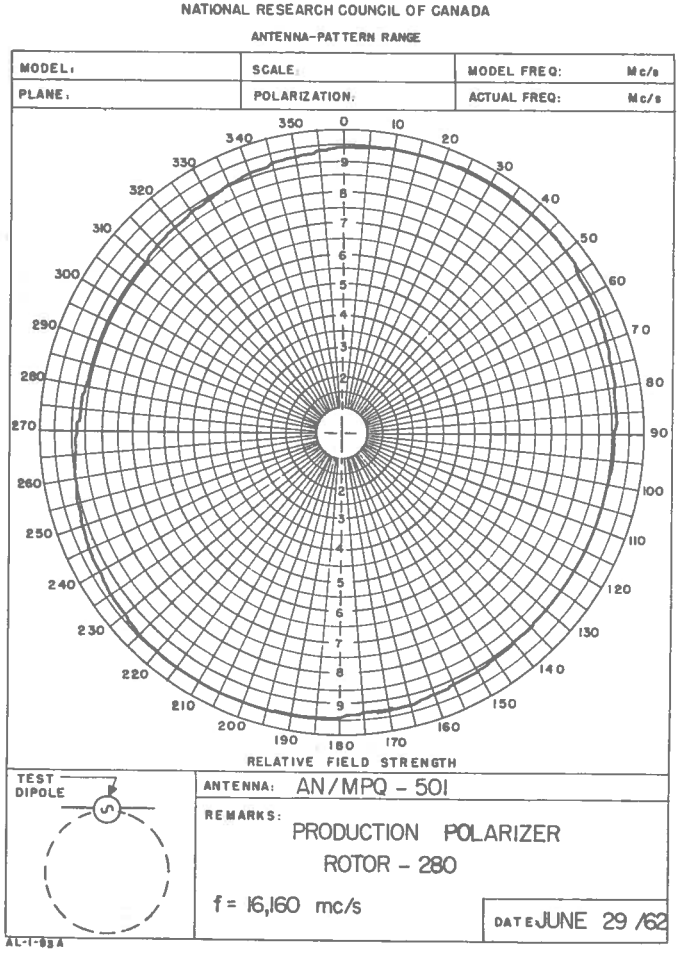

Fig. 45 Polarization pattern. Rotor = 280°, $f = 16,160$ mc/s

was dried from a state of average humidity. It may be that dimensional or other differences exist between the production polarizer and the others tested previously, or it may be that performance can be improved through a minor change in polarizer positioning.

Acknowledgment

The authors are indebted to Mr. James Barnes, Mr. Hugh Gribbon, and Mr. Lorne Woods for handling a number of mechanical problems associated with the mounting and maintenance of the scanner, and with the manufacture of various devices used during the tests, and to Mr. Brian Bradley for the maintenance of our recording equipment, as well as for certain modifications thereto. Mrs. M. Steen prepared many of the drawings for this report.

References

1. Canadian Army Equipment Specification, Radar Set, AN/MPQ-501 CA-E. 106, Issue 1, 14 September, 1960
Amendment 1, 3 October, 1960
Amendment 2, 15 February, 1961

2. "Provisional Specification for the Polarizer for AN/MPQ-501", National Research Council (Confidential) June 1958

3. "Pattern and Gain Measurements on the Modified CB Antenna", W.A. Cumming and E.P. Deloli, NRC/REED Report ERB-335 (Confidential), May 1954

4. "Testing of the CAL Prototype of the CB Antenna for Patterns, Gain and Beam Position", G.C. McCormick, NRC/REED Report ERB-433 (Confidential), July 1957

5. "A Microwave Antenna with Rapid Sawtooth Scan", J.S. Foster, Can. J. Phys. 36: 1652-1660, 1958

6. "A Mechanically Simple Foster Scanner", R.C. Honey and E.M.T. Jones, IRE Trans. AP-4: 40-46, 1956

7. "A Device for Locating the Phase Center of an Antenna", G.C. McCormick and D.M. Fellows, Bulletin of the Radio and Electrical Engineering Division, NRC, vol. 11, no. 3, 1961, p. 5

8. "The Design and Calibration of Microwave Antenna Gain Standards", W.T. Slayton, Naval Research Laboratory, Washington, D.C., Report No. 4433, November 1954

APPENDIX I

RESUMÉ OF ANTENNA DESIGN

An important design change was made in the transition from the McGill-NRC antenna to the NRC-CAL model. This was the replacement of intermeshing teeth with chokes and barriers. It was found that the matching of the unity-coupled tee which connects the slotted waveguide region to the rotor-stator region would require a longitudinal iris if the original separations were retained. The rotor-stator separation was therefore changed from 0.322" to 0.172", thereby permitting a match without the use of an iris. It was found expedient to divide the 90° bends into two 45° sections. The design follows that given in the "Waveguide Handbook", Radiation Lab. Series, vol. 10, 1951, p. 316. Data were obtained with K_u-band test sections in the design of both the tee and the bend. Data for the bend were also obtained with a test section scaled to X-band. These measurements indicate that the bends and the tee were matched to better than a VSWR of 1.06 over the band. Measurement indicated further that the power flowing past the choke in the rotor was more than 30 db down over the frequency band. Diagrams of the tee are shown in Fig. 46 and of the bends in Fig. 47.

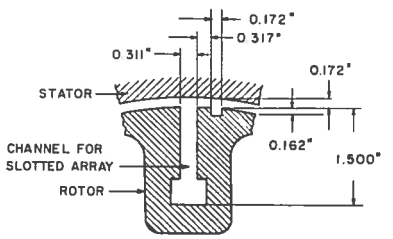

Fig. 46 Unity coupled tee. The choke barrier prevents transmission of energy past it

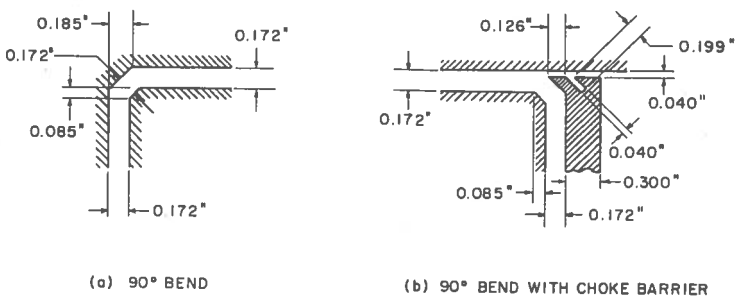

Fig. 47 90° bends: (a) in the stator region, (b) with choke barrier between rotor and stator

The inclusion of an elongated wedge-shaped parallel-plate region in the production model resulted in a scanner with an approximately symmetrical scan. The interior regions of the scanner in relation to the reflector are shown developed in Fig. 3.

With the change in scan geometry the reasons for a good horn match became greater. In addition, the horn separation was changed slightly to produce a beam separation closer to the nominal 40 mils. The redesigned horn assembly is shown in Fig. 48.

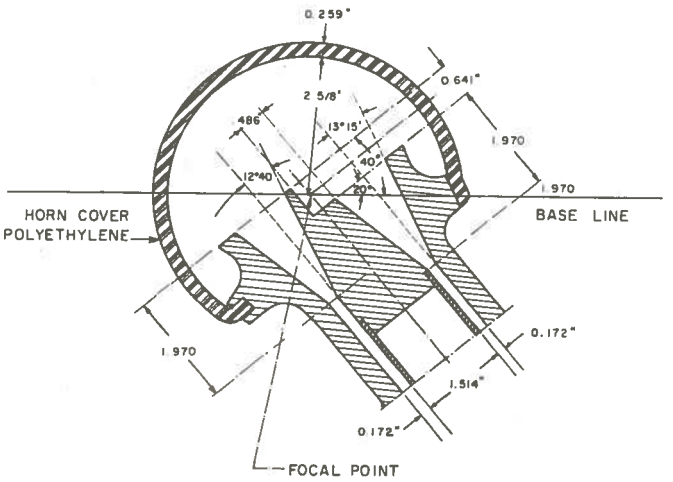

Fig. 48 Horn assembly

The slotted array was designed to produce an incomplete Gaussian amplitude distribution with a taper ratio of 5.0*. The ideal level of the first side lobe corresponding to this distribution is -28.4 db.

* "Fourier Transformer in Aerial Theory, Part V", J.F. Ramsay, The Marconi Review, vol. X, no. 4, 1947, p. 157

APPENDIX II

THE RADAR SAFE DISTANCE FOR AN/MPQ-501

Much work in recent years has led to the establishment of a power flux density of 0.01 watts/cm^2 as the maximum safe level to which personnel working in the vicinity of radar equipments may be exposed. Taking account of the report by Overman*, and other considerations, the following formulas using the above criterion may be applied for the region in front of the AN/MPQ-501 antenna.

a) Safe power at all distances : 75 watts, average

b) Safe distance (in feet) : $24\ W^{\frac{1}{2}}$ (W = average power in watts)

Personnel working at the rear of the antenna are exposed directly to the spill-over under the reflector. A calculation based on the primary patterns leads to a maximum power density in watts/cm^2 to the rear of 2×10^{-5} W, where W is the average radiated power in watts. This level appears to be safe for present and contemplated powers.

---

* "Simplified Formula for Estimating Safe Distances in Radar Beams", H.S. Overman, Naval Weapons Laboratory, U.S., Tech. Memo No. W-27/59, November 1959

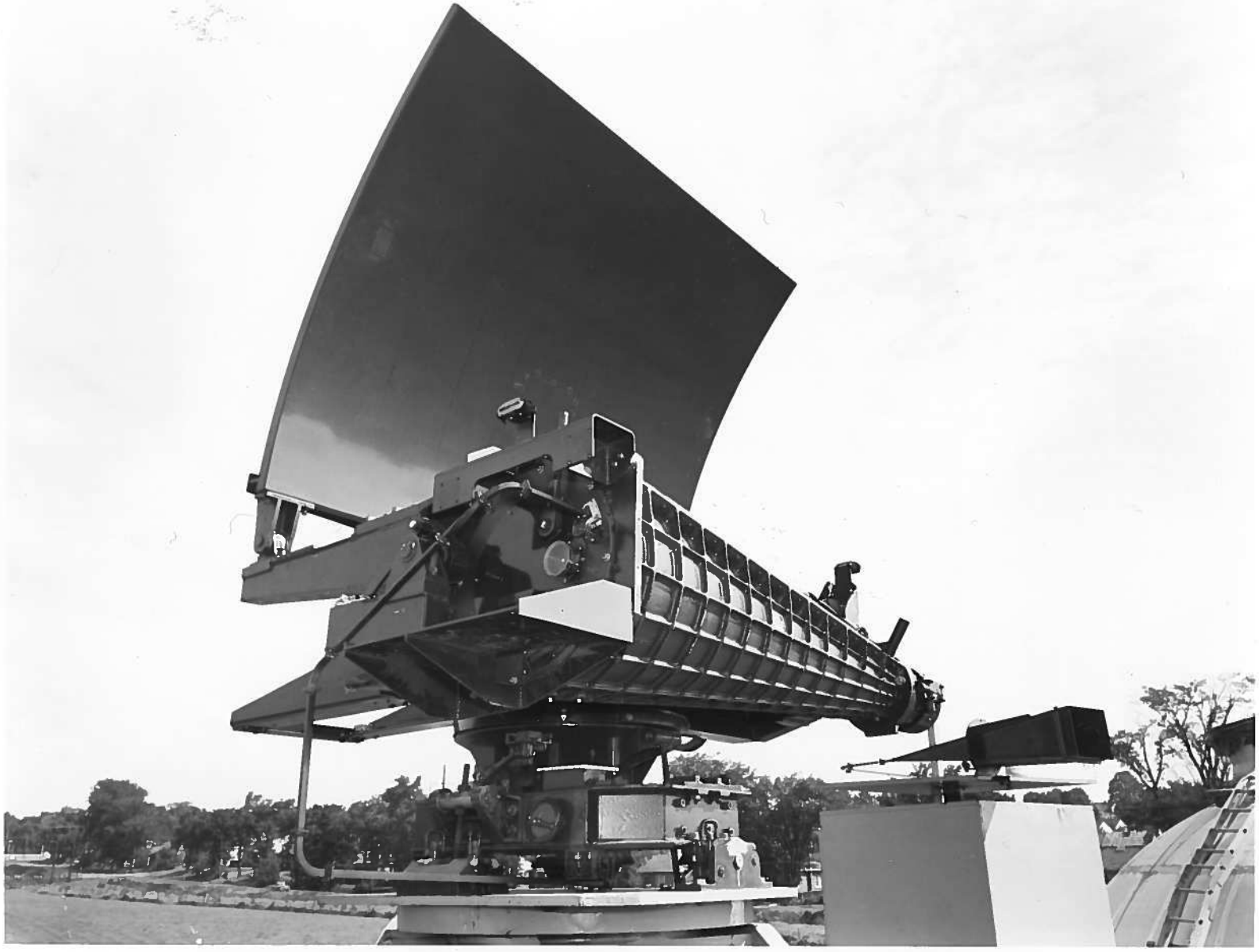

Plate I — The AN/MPQ-501 antenna mounted for electrical tests

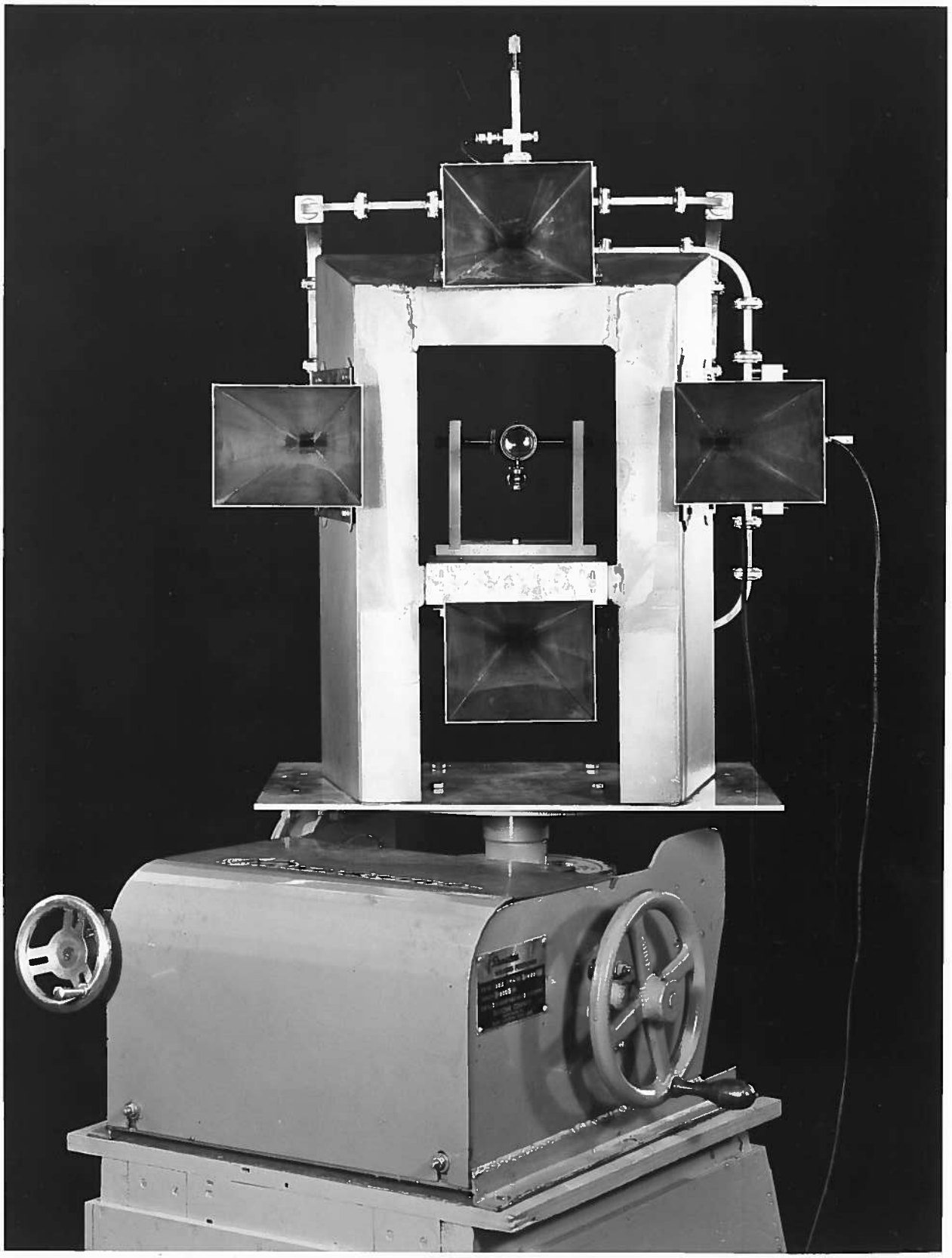

Plate II — Apparatus for the location of the phase center